THERMODYNAMIC MODELING AND ANALYSIS OF MICRO GAS TURBINE AS A RANGE EXTENDER IN ELECTRIC VEHICLES WITH THE EVALUATION OF BATTERY PACK SIZING

By

Syed Umer Bin Arif
Reg # 00000170424
Session 2016-2018

Supervised by
Dr. Adeel Javed

A Thesis Submitted to the US Pakistan Centre for Advanced Studies in Energy in partial fulfilment of the requirements of the degree of

MASTERS of SCIENCE in

THERMAL ENERGY ENGINEERING

US-Pakistan Centre for Advanced Studies in Energy (USPCAS-E)

National University of Sciences and Technology (NUST) H-12,

Islamabad 44000, Pakistan

THESIS ACCEPTANCE CERTIFICATE

Certified that final copy of MS/MPhil thesis written by Syed Umer Bin Arif (Registration No. 00000170424), of U.S.-Pakistan Centre for Advanced Studies in Energy has been vetted by undersigned, found complete in all respects as per NUST Statues/Regulations, is within the similarity indices limit and accepted as partial fulfillment for the award of MS/MPhil degree. It is further certified that necessary amendments as pointed out by GEC members of the scholar have also been incorporated in the said thesis.

Signature: _____

Name of Supervisor   Dr. Adeel Javed_____

Date: _____

Signature (HoD): _____

Date: _____

Signature (Dean/Principal): _____

Date: _____

<u>Certificate</u>

This is to certify that work in this thesis has been carried out by **Mr. Syed Umer Bin Arif** and completed under my supervision in, US-Pakistan Center for Advanced Studies in Energy (USPCAS-E), National University of Sciences and Technology, H-12, Islamabad, Pakistan.

Supervisor:

Dr. Adeel Javed
USPCAS-E
NUST, Islamabad

GEC member # 1:

Dr. Muhammad Bilal Sajid
USPCAS-E
NUST, Islamabad

GEC member # 2:

Dr. Dr. Muhammad Zubair
USPCAS-E
NUST, Islamabad

GEC member # 3:

Dr. Muhammad Majid Ali
USPCAS-E
NUST, Islamabad

HoD- (dept): _____

Principal/ Dean

Dr. Zuhair S. Khan
USPCAS-E
NUST, Islamabad

List of Publications

Paper presented as follows

1. Title: "Design and analysis of micro gas turbine as a range extender in electric vehicles"
   Conference: The International Conference on Renewable, Applied and New Energy Technologies
   Date: 19-22 November 2018
   Venue: Air University, Islamabad.

2. Title: "Minimization of Energy crisis by introducing Range Extender in Electric Vehicles – Evaluation of battery pack sizing and Engine Optimization"
   Conference: 38th All Pakistan Science Conference
   Date: 10-11 December 2018
   Venue: Punjab University, Lahore.

Acknowledgement

I would like to thank my creator Almighty Allah, the Gracious, and the beneficent, whose benediction bestowed upon me, provided me the ample opportunity and guided me throughout this work at every step.

I would like to express special gratitude to my supervisor Dr. Adeel Javed for his priceless help and tremendous support. I would also like to thank Dr. Majid Ali, Dr. Muhamamd Bilal Sajid and Dr. Muhammad Zubair for their guidance. I am grateful to my beloved parents, Mr. and Mrs. Arif, my wife Mrs. Umer, my sister who nurtured me and continued to support me throughout in every step of my life.

During my thesis session, I always stayed at my In-Laws' residence, I am really thankful for their support and facilities which were given to me.

Abstract

Range extenders based on micro gas turbine (MGT) technology are being promoted in electric vehicles (EV) in order to reduce the battery size and extend the driving range. MGT offers higher power density, fuel flexibility, lower weight and good efficiency (with recuperation) compared to conventional reciprocating engines. MGT facilitates a relatively smaller battery pack, which ultimately can reduce the capital and maintenance cost of electric vehicles. Despite its advantages, MGT incurs small-scale design issues related to component performance, heat transfer between hot and cold sections and manufacturing limitations. In this research project, the design of an MGT has been studied simultaneously with the battery bank size and charging time analogy with an aim to evaluate their conjoint operation. In addition, the influence of MGT small-scale effects on battery pack recharging has been presented. For the study, Gas Turbine Simulation Program (GSP) has been extensively used together with detailed battery pack calculations. Comparison between sizing of the battery and MGT design is a critical outcome of this research.

Keywords: micro gas turbine, range extender, electric vehicles, battery size, charging time, design and performance, Gas Turbine Simulation Program (GSP)

Contents

List of Figures

List of Tables

Nomenclature

CD   Throat drag coefficient

cr   Charge Rate [cr]

CV   Velocity coefficient

CX   Thrust coefficient

dc   Diameter of cell [mm]

E20%   Battery energy at SOC 20% [kWh]

Eb   Energy of battery pack [kWh]

Eb   Battery energy [kWh]

Ec   Energy of one cell [Wh]

Ed   Energy Density of one cell [Wh L-1]

$E_{ON,engine}$ Energy required when Engine is ON [kWh]

Er   For 100%, battery needs [kWh]

Et   Total energy required [kWh]

hc   Height of cell [mm]

hrel   Relative humidity

Ib   Current of the battery pack [A]

Ic   Current of one cell [A]

ma   Design mass flow

Nc   Number of cells in series [cells]

Nc   Compressor rotor speed

Ns   Number of series in parallel [series]

Nt   Number of total cells [cells]

Nt   Turbine rotor speed

P   Engine Power [kW]

Pa   Ambient pressure

PC   Power Consumption [Wh km-1]

PLb   Combustor pressure loss

PLr,1   Recuperator pressure loss flow 2

PLr,2   Recuperator pressure loss flow 1

PR1   Pressure ratio at inlet

Qb   Capacity of battery pack [Ah]

Qc   Capacity of one cell [Ah]

R   Driving Range [km]

$R_{OFF,engine}$ Travel Distance for OFF engine [km]

$R_{ON,engine}$ Travel Distance for ON Engine [km]

s   Car average speed [km hr-1]

SOC   State of charge

SOCr   Recharging start at SOC

t   Time of charging [hr]

t   Time of charging [min]

Ta   Ambient temperature

TIT   Turbine inlet temperature

$t_{OFF,engine}$ Travel Time for OFF engine [min]

$t_{ON,engine}$ Travel Time for ON Engine [min]

tt   Total charging time for ON Engine [min]

Vb   Voltage of battery pack [V]

vc   Volume of one cell [mm3]

vc   Volume of one cell [L]

Vd   Avg. Discharge Voltage of one cell [V]

wb   Weight of batteries [kg]

wc   Weight of one cell [g]

wp   Weight of battery pack [kg]

ηb   Efficiency combustor

ηc   Efficiency compressor

ηr   Effectiveness recuperator

ηt   Efficiency turbine

Subscript

c   Cell / compressor

b   Battery bank / combustor

p   Battery pack

r	Recuperator / required
d	Discharge
t	Turbine / total
D	Drag
V	Velocity
X	Thrust
ON,engine	ON engine mode
OFF,engine	OFF engine mode

Chapter 1

INTRODUCTION

1.1. Background

An EV offers efficiency and sustainability, application of diversified fuel sources, renewable energy integration and pollution free transport substitute of conventional gasoline based automobiles [1-5]. Owing to their environmentally friendly characteristics, the developed world is gradually encouraging a shift from conventional internal combustion (IC) engine based automobiles; including hybrid electric vehicles (HEV) to battery electric vehicles (BEV). Automotive sector has continuously been launching new EV models [6, 7]. According to ref. [8], the EV stock has exceeded 3 million units in 2017. Nonetheless, EVs still only represent 0.3% of the global car fleet. The report also mentions that China is the largest EV market globally, followed by Europe and the US, while Norway is the global leader in terms of market share, with 40% in 2017. The ultimate aim is to make all passenger vehicles emission-free by 2050 [9, 10]. For example, the USA is targeting electrification of automobiles by 2025. Europe has pledged to reduce the environmental impact of automobiles by 40% by 2030. Germany is about to become the first major country to set an official deadline for a ban on gas-powered cars. Similarly, India has started to produce electric vehicles to minimize consumption of fossil fuels. Simultaneously, the government of Pakistan is welcoming the HEV technology with tax relaxations in order to fight global warming and minimize fuel consumption in the transport sector. Considering half to one-third of energy used by IC engines, EVs have allowed to reduce the global well-to-wheel $CO2$ emission savings of 29.4 Mt CO_2 in 2017, while abating pollutant emission savings in high exposure urban environments [8].

1.1.1. Battery Packs

Lithium-ion based battery packs are expected as the technology of choice for the next decade [8]. The critical challenges to extend the market share of electric vehicles (EVs) are performance, safety and reliability. These issues are closely linked to the energy storage system in the

EVs. Lithium-ion batteries have revolutionized the EV industry to become the preferred battery choice for EVs. This is due to their outstanding characteristics including high voltage, high energy density, long cycle life, low self-discharge rate, high charging and discharging rate capability. In EVs, Lithium-ion cells are connected in series and/or parallel to deliver the required power to the traction motor and auxiliary systems. However, due to the operating environment of EVs, the Lithium-ion battery may not perform to the best of its ability when integrated into an EV battery pack. [11].

Battery pack is a key component in any EV for electrical energy storage. More and more batteries are being produced with an increase in the demand of EVs. In addition, the charging mechanism of EVs has been a point of focus for the stakeholders including producers and consumer. Developers have tried to facilitate battery charging through different methods including plug-in chargers for homes, instant chargers and on-board charging devices, also known as range extenders. Moreover, optimization models have been studied to identify battery range of minimum requirement and its effect on the service range of charging stations, and extreme trips [12]. A pictorial outlook of battery pack is displayed in Fig. 1.

Figure 1. EV Battery Pack

1.1.2. Range Extender

Range Extenders are used to enhance driving range of electric vehicles. The most commonly used range extenders are internal combustion (IC) engines, fuel-cells, and micro gas turbines (MGT). Range Extender also known as Auxiliary Power Unit (APU) provides better solution to the limited range and overpriced cost of electric vehicle. Range extended electric vehicle (REEV) operates essentially as a BEV until their batteries become depleted; at this point they utilize an Auxiliary Power Unit (APU) that draws energy from liquid or gaseous fuel and provides electricity to charge batteries, allowing the vehicle to continue operating [13-18]. Compared to conventional hybrid vehicles, REEVs could significantly reduce fuel consumption and emissions. Compared with pure electric vehicles, REEVs could increase the driving range, therefore it is seen as one of the most promising technological bridges between the vehicles of today and the sustainable concepts of tomorrow [19]. A typical REEV powertrain is based on the arrangement given in Fig. 2, which is also known as a series hybrid powertrain.
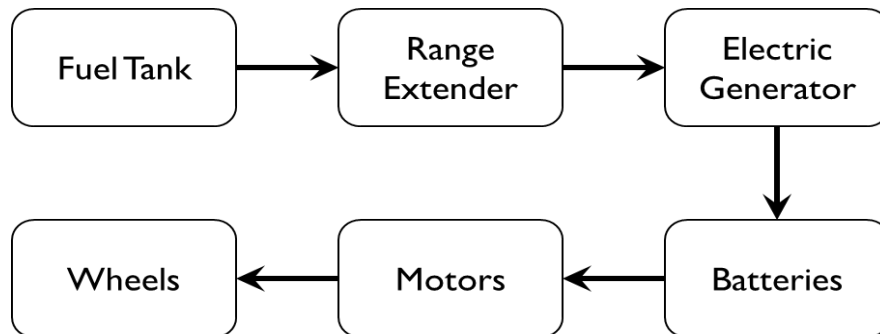
Figure 2. Series hybrid powertrain (REEV configuration)

Range Extender draws energy from fuel tank and run electric generator which charges batteries to turn electric motors. Motors are used to power wheels.

1.1.3. Micro Gas Turbine Technology

The main requirements for a range extender are compactness, lightweight to minimize the vehicle efficiency penalty of carrying dead weight and less maintenance. Consequently, small turbocharger based MGTs have the potential to be a range extender in EV [20-26].

As a range extender, MGT offers a capable solution for standalone electricity generation systems and onboard charging devices for Electric Vehicles. This study focuses the design and analysis of micro turbine to enhance driving ranges and minimizes cost for batteries in an electric vehicle.

Famous names in the production of MGTs are MTT, Delta motorsports, Bladon Jets, Mitsubishi and Capstone. The developers have claimed 25-30% electrical efficiency. Figure 3 shows a MGT range extender developed by Mitsubishi Heavy Industries (MHI) for EV application.

MGT as a range extender provides potential solution to extend the driving range of electric
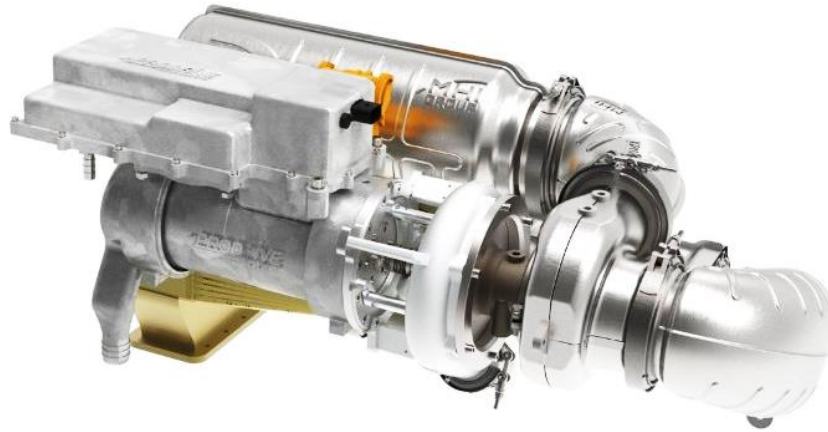
Figure 3. A turbocharger based MGT developed by MHI Group

vehicles. They provide electricity to recharge batteries while driving and allow the vehicle to continue operating [27].

1.1.4.   Nature of Issues

Presently, electric vehicles carry large battery packs with them to extend their driving range. These batteries are expensive to maintain and take a few hour time to recharge. On average, people drive short distances per day, so carrying expensive and heavy batteries is not a viable solution. Large battery packs also increase the cost of vehicle. Automobiles, therefore, need more electrification instead of incorporation of large battery packs in order to produce lighter and cost-effective vehicles. An MGT allows reduction in the cost of batteries and provide the power on need basis. The miniature size of MGT, however, means smaller and fast turning turbomachinery. The main challenges faced by small-scale turbomachinery are: (1) high viscous losses due to low Reynolds number and large relative surface roughness, (2) manufacturing and assembly constraints resulting in large relative tip-clearance and thicker blades mainly, (3) rotordynamic issues, and (4) large heat flux from hot to cold sections due to shorter distances between components [27]. Moreover, a strategy is not available to design MGTs as range extenders in conjunction with the battery bank size and charging time.

1.1.5.   Scope of Work

The goal of this study is to propose a strategy to design MGTs for range extender application in EVs. The foremost aim is to understand the complex relationship between the MGT thermodynamic cycle, battery bank size and charging time involved in the complete system. The strategy requires an understanding of the system and setting up a novel methodology in order to devise and match such automotive systems of the future. The main objectives are: (1) calculating the battery charging time required (30 min assumed in this case) considering the power consumption at different speeds of the EV, (2) conduct a sizing of EV battery pack considering a relatively smaller drive range up to 100 km, (3) design of a suitable MGT thermodynamic cycle considering various parameters, (4) estimate the effect of component performance variation on the battery bank and charging time analogy, and finally (5) define a unified guideline for optimum sizing of the range extender system for an EV application. The Tesla Model S P85D has been considered as the hypothetical test case in this study. This EV had been designed for a driving range of 510 km having a battery pack of 85 kWh. The battery pack weighs 540 kg, which is about 1/4th of the total weight of the car.

1.1.6.   Gas Turbine Simulation Program

 The Gas Turbine Simulation Program (GSP) has been developed by NLR, Netherlands. It is a tool to analyze gas turbine engine performance with the help of component based modeling environment tool. It has component-by-component approach which allows virtual modeling for any type of system. It facilitates both steady state and transient simulations for any kind of gas
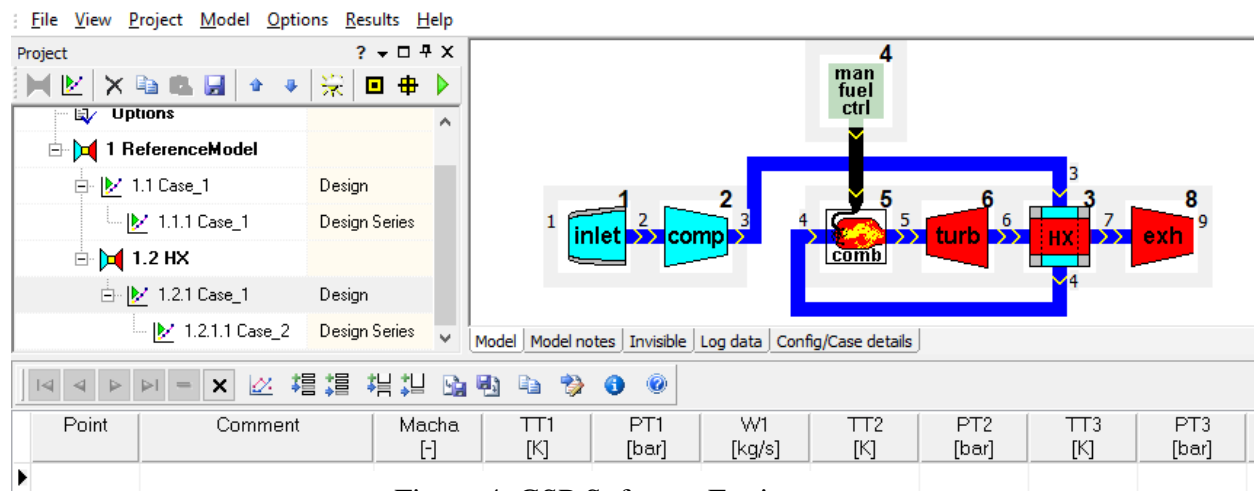
Figure 4. GSP Software Environment

turbine configuration. To allow analyzing the performance of a "physically-based" component, GSP gives the possibility to perform off-design simulations. The simulation is based on one-dimensional modeling of the processes in the different gas turbine components with thermodynamic relations and steady-state characteristics (component maps). GSP can be used to calculate pressures, gas temperatures, composition and velocities at relevant engine stations from measured engine data. GSP software environment is shown in Fig. 4.

GSP created a gas turbine model by organizing different predefined components (inlet, compressors, combustors, turbines, combustors, recuperator and exhaust nozzles). For further process, the GSP output is investigated in Microsoft Excel. In order to benefit this study, several performance models of the MGT have been considered using the NLR Gas Turbine Simulation Program (GSP). The GSP model has been used to generate performance data of a MGT with power outputs of 15-60 kW.

1.2. Relevance to National Need

In Pakistan, transportation and traveling sector is the 2nd largest fuel consumer which is causing pollution and high cost of delivery goods as well as expensive traveling through personal conveyance. Government is emphasizing production / import of hybrid electric vehicles to reduce energy bill and pollution. This project will contribute towards further understanding of hybrid EV and assist in designing elegant MGTs for automotive application. This project can be further extended into prototyping of MGT in Pakistan. MGT installed electric vehicle will provide economical and environment friendly ride within the city as well as on highways.

1.3. Methodology

In the first part of the study, battery pack calculation and charging time analogy have been modeled simultaneously to meet the 100 km driving range and 30 min of charging time. The performance output curves for driving range and charging time vs vehicle speed are obtained as a result. Moving on to the second phase, MGT modeling and simulations have been done on Gas Turbine Simulation Program (GSP) by considering CAPSTONE C30 as reference MGT [25]. This is followed by cycle optimization and simulating the influence of component characteristics on overall MGT design.

From these results, both the battery Pack and MGT have been matched together for multiple compatibilities. Figure 4 illustrates the methodology followed in the study.
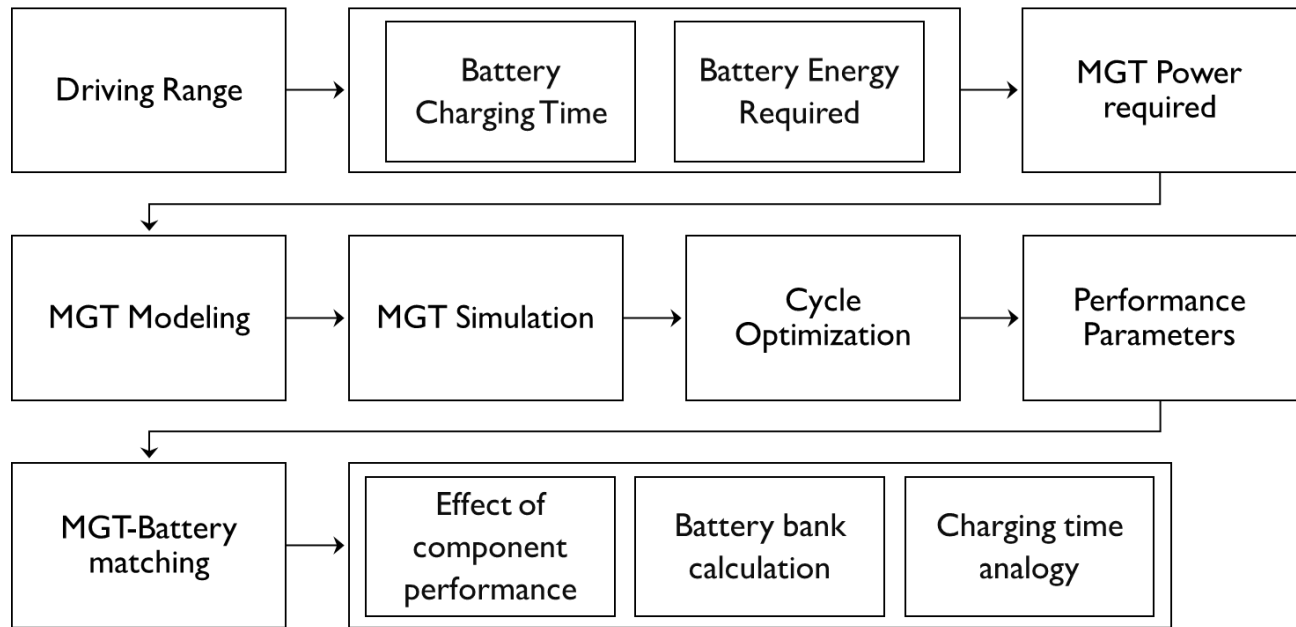
Figure 5. Methodology followed in the study

1.4. Thesis Outline

This thesis is split into 6 chapters.

Chapter 1 focuses on motivation and background of this research project which consist of introduction of battery packs of EV, range extenders, nature of issues in electric vehicles, scope of work, working and application of MGT and work methodology.

Chapter 2 includes detailed literature review of micro gas turbine and its problems in small scale designing and operation.

Chapter 3 consists of battery bank calculation for EV and it charging time analogy with respect to designed MGT.

Chapter 4 includes MGT designing and simulation and its impact on battery bank size and driving range.

Chapter 5 comprises of performance of component evaluation of MGT which influences battery pack size for EV and describes how it influence driving ranges for different applications.

Chapter 6 This chapter focuses experimental setup work which was done in Arizona State University during exchange research program. Whole setup was built in Thermo Fluids Lab under the supervision of Dr. Tae Woo Lee.

References

[1] IEA. Global EV outlook: understanding the electric vehicle landscape to 2020. International Energy Agency; 2013.

[2] Lund. PD., Lindgren, J., Mikkola, J., Salpakari, J., 2015. Review of energy system flexibility measures to enable high levels of variable electricity. Renewable and Sustainable Energy Reviews, Vol. 45, P. 785-807.
https://doi.org/10.1016/j.rser.2015.01.057.

[3] Salpakari, J., Rasku, T., Lindgren, J., Lund, PD., 2017. Flexibility of electric vehicles and space heating in net zero energy houses: an optimal control model with thermal dynamics and battery degradation. Journal of Applied Energy, Vol. 190, P. 800-812.
https://doi.org/10.1016/j.apenergy.2017.01.005.

[4] Shokrzadeh, S., Bibeau, E., 2016. Sustainable integration of intermittent renewable energy and electrified light-duty transportation through repurposing batteries of plug-in electric vehicles, Journal of Energy, Vol. 106, P. 701-711.
https://doi.org/10.1016/j.energy.2016.03.016.

[5] Wu. X, Hu, X., Teng, Y., Qian, S., Cheg, Ru., 2017. Optimal integration of a hybrid solar-battery power source into smart home nanogrid with plug-in electric vehicle. Journal of Power Sources, Vol. 363, P. 277-283. https://doi.org/10.1016/j.jpowsour.2017.07.086.

[6] Wiang, N., Tang, L., Pan, H., 2019. A global comparison and assessment of incentive policy on electric vehicle promotion, Journal of Sustainable Cities and Society, Vol. 44, P. 597-603.
https://doi.org/10.1016/j.scs.2018.10.024.

[7] Nie, YM, Ghamami, M., Zockaie, A., Xiao. F., 2016, Optimization of incentive polices for plug-in electric vehicles, Transportation Research Part B Methodological, Vol. 84, P. 103-123.
https://doi.org/10.1016/j.trb.2015.12.011.

[8] IEA. Global EV outlook 2018. International Energy Agency; 2018.

[9] Article: "All new cars mandated to be electric in Germany by 2030". Available (online)
https://electrek.co/2016/06/14/all-new-cars-mandated-electric-germany-2030/

[10] Article: "Europe's attempts to spark an electric vehicle revolution". Available (online)
https://www.euractiv.com/section/electric-cars/news/europes-attempts-to-spark-electric-vehicle-revolution/

[11] Lip Huat Saw, Yonghuang Ye, Andrew A.O. Tay. Journal of Cleaner Production
Volume 113, 1 February 2016, Pages 1032-1045. Integration issues of lithium-ion battery into electric vehicles battery pack.

[12] Shi, X., Pan. J., Wang, H., Cai, H., 2019. Battery electric vehicles: what is the minimum range required? Journal of Energy, Vol. 166, P. 352-358.
https://doi.org/10.1016/j.energy.2018.10.056.

[13] Arav B, Shulman R, Dooun V. Basic concepts for forcing of low-power micro turbine generators. Procedia Eng 2016; Vol 150: P. 1384-1390.

[14] Arav BL, Shulman R, Kozminykh VA. Refinement of hybrid motor-transmission set using micro turbine generator. Procedia Eng 2015; Vol 129: P. 166-170.

[15] Christodoulou F, Giannakakis P, Kalfas AI. Performance benefits of a portable hybrid micro-as turbine power system for automotive applications. J Eng Gas Turbines Power 2010; Vol 133(2): 022301 (Oct 29, 2010) (8 pages)

[16] Feneley AJ, Pesiridis A, Mahmoudzadeh Andwari A. Variable geometry turbocharger technologies for exhaust energy recovery and boosting-a review. Renew Sustain Energy Rev 2017; Vol 71: P. 959-975.

[17] Ghanaati A, Mat Darus IZ, Farid M, Said M, Mahmoudzadeh Andwari A. A mean Value model for estimation of laminar and turbulent flame speed in spark-ignition engine. Int J Automot Mech Eng 2015; Vol 11: P. 2224-2234. DOI: 10.15282/ijame.11.2015.5.0186

[18] Mahmoudzadeh Andwari A, Pesiridis A, Karvountzis-Kontakiotis A, Esfahanian V. Hybrid electric vehicle performance with organic rankine cycle waste heat recovery system. Appl Sci 2017; Vol 7(5): P. 437.

[19] Song K, Zhang J, Zhang T, Design and Development of a Pluggable PEMFC Extended Range Electric Vehicle. Second International Conference on Mechanic Automation and Control Engineering (MACE), 2011. DOI: 10.1109/MACE.2011.5987138

[20] Abagnale C, Cameretti MC, De Robbio R, Tuccillo R. CFD study of a MGT combustor supplied with syngas. Energy Procedia 2016; 101:933e40

[21] Almasi A. Bright future of micro-turbines: nuclear emergency cooling and miniature generator. Aust J Mech Eng 2013;11(2): P. 169-175. DOI: 10.7158/M11-828.2013.11.2

[22] Bakalis DP, Stamatis AG. Performance simulation of a hybrid micro gas turbine fuel cell system based on existing components. 2011. P. 171-179 (54648). doi:10.1115/GT2011-45834.

[23] W. J. P. Visser, S. A. Shakariyants, M. Osostveen. "Development of a 3 kW Microturbine for CHP Applications" DOI: 10.1115/1.4002156 J. Eng. Gas Turbines Power 133(4), 042301 (Nov 22, 2010) (8 pages)

[24] Article: "Delta launches MiTRE Range Extender" by Deltra Sports. Published online https://www.delta-motorsport.com/news/2016/delta-launches-mitre-range-extender/

[25] AlfredoGimelli, RanieroSannino. "Thermodynamic model validation of Capstone C30 micro gas turbine". Volume 126, September 2017, Pages 955-962. https://doi.org/10.1016/j.egypro.2017.08.184

[26] Tate ED, Harpster MO, Savagian PJ, The Electrification of the Automobile: from Conventional Hybrid, to Plug-in Hybrids, to Extended Range Electric Vehicles. SAE paper 200801-0458, 2008. & January 2009. SAE International Journal of Passenger Cars - Electronic and Electrical Systems 1 Vol 1: P. 156-166.

[27] Tate ED, Harpster MO, Savagian PJ, The Electrification of the Automobile: from Conventional Hybrid, to Plug-in Hybrids, to Extended Range Electric Vehicles. SAE paper 200801-0458, 2008. & January 2009. SAE International Journal of Passenger Cars - Electronic and Electrical Systems 1 Vol 1: P. 156-166

Chapter 2

LITERATURE REVIEW

2.1. Introduction

A gas turbine, also called a combustion turbine, is a type of continuous combustion, internal combustion engine. There are three main components,

- An upstream rotating gas compressor
- A downstream turbine on same shaft.
- A combustion chamber or area, called a combustor, in between compressor and turbine

Gas turbine was invented by an Englishman, John Barber in 1791. This invention opened new door in engineering horizon and attracted technologist of every time to step in for new developments.

In an ideal gas turbine, gases undergo four thermodynamic processes:

- an isentropic compression
- an isobaric (constant pressure) combustion
- an isentropic expansion
- heat rejection
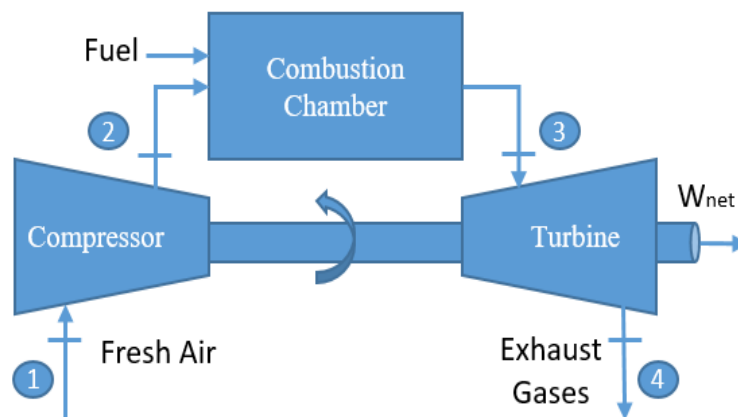
Figure 6: Cycle of GT

Together, these make up the Brayton cycle [1].

In a real gas turbine, mechanical energy is changed irreversibly (due to internal friction and turbulence) into pressure and thermal energy when the gas is compressed (in either a centrifugal or axial compressor). Heat is added in the combustion chamber and the specific volume of the gas increases, accompanied by a slight loss in pressure. During expansion through the stator and rotor passages in the turbine, irreversible energy transformation once again occurs. Fresh air is taken in, in place of the heat rejection.
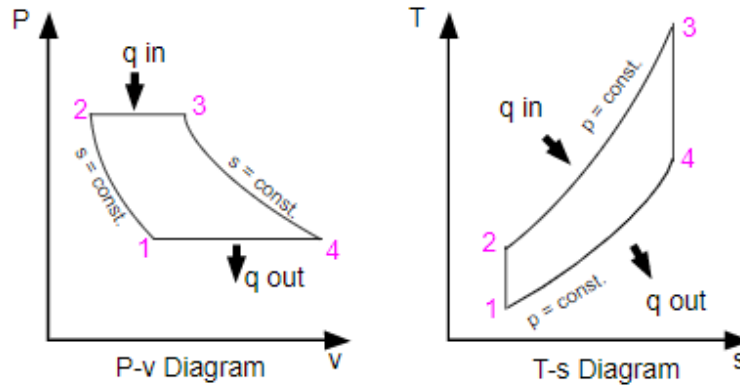
Figure 7: Thermodynamic Cycle of GT [1]

By scaling down a conventional gas turbine we can build micro gas turbine which are well-known in distributed power and combined heat and power applications, and are very promising for powering hybrid electric vehicles. Basic principles of micro gas turbine are based on micro-combustion.

These MGTs are widely used in:
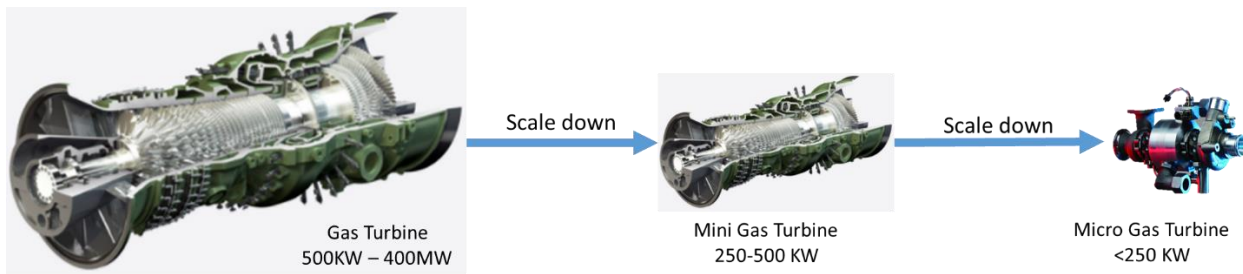
Figure 8: Gas turbine scaling down to Micro GT

- Power Generation
- Micro-Scale Power Generation

MGTs range from hand held units producing less than a kilowatt, to commercial sized system that produce tens or hundreds of kilowatts [2]. In this study, we are designing micro sized gas turbine

to generate electricity for battery charging.

2.2. Thermodynamic Analysis

A set of parameters was used to run GSP simulations in order to achieve maximum possible power output. A thermodynamic analysis for Micro Gas Turbine is presented with the help of following equations. [3] Starting with first law analysis of Brayton Cycle [4];

$$\frac{dE_{cv}}{dt} = \dot{Q}_{in} - \dot{W}_{out} + \sum_{in} \dot{m}(h + \frac{v^2}{2} + gz)_{in} - \sum_{out} \dot{m}(h + \frac{v^2}{2} + gz)_{out} \qquad 01$$

The cycle efficiency is

$$\eta = \frac{\text{net work output}}{\text{heat supplied}} = \frac{C_p(T_3 - T_4) - C_p(T_2 - T_1)}{C_p(T_3 - T_2)} \qquad 02$$

Making use if this isentropic p-T relation, we have

$$\frac{T_2}{T_1} = r^{\frac{(Y-1)}{Y}} = \frac{T_3}{T_4}$$

Where r is the pressure ratio $p_2 / p_1 = r = p_3 / p_4$. The cycle efficiency is then readily shown to be given by

$$\eta = 1 - \left(\frac{1}{Y}\right)^{\frac{(Y-1)}{Y}} \qquad 03$$

The efficiency thus depends only on the pressure ratio and the nature of the gas.

The specific work output W, upon which the size of plant for a given power depends, is found to be a function not only of pressure ratio but also of maximum cycle temperature T*3*. Thus

$$W = c_p(T_3 - T_4) - c_p(T_2 - T_1)$$

Which can be expressed as

$$\frac{W}{c_p T} = t\left(1 - \frac{1}{r^{\frac{(Y-1)}{Y}}}\right) - \left(r^{\frac{(Y-1)}{Y}} - 1\right) \qquad 04$$

To enhance cycle efficiency, a heat exchanger has been added to the system whose effectiveness is

12
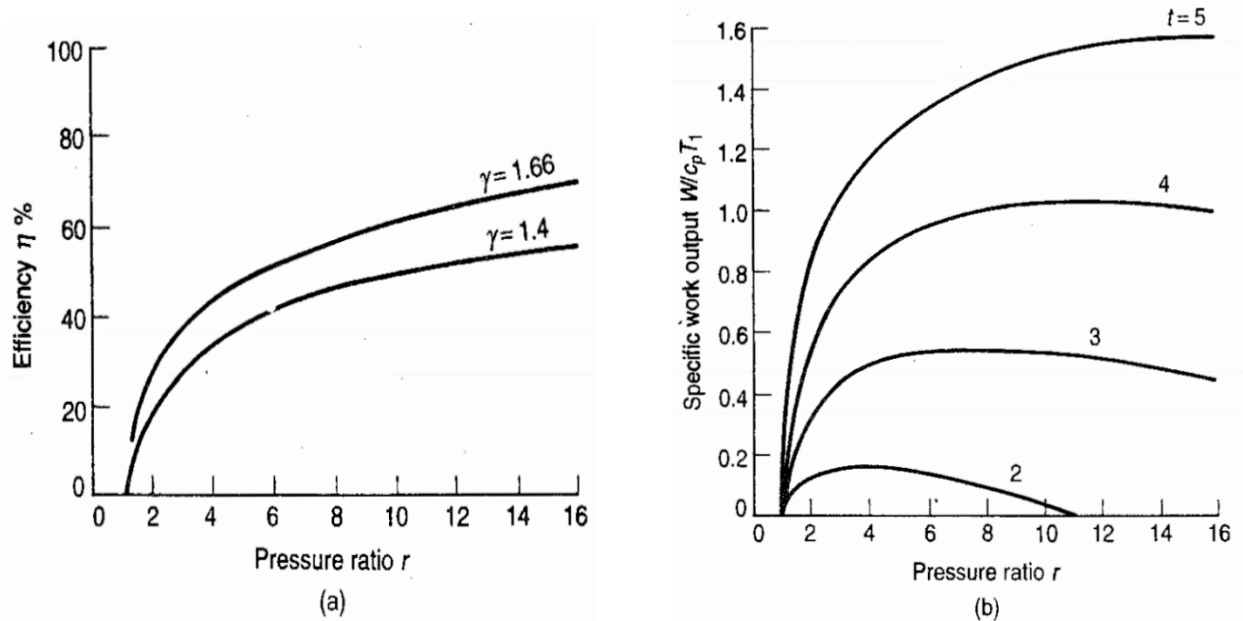
Figure 9: Simple cycle Efficiency (a) and Specific work output (b) vs Pressure Ration [4]

$$\text{effectiveness} = \frac{T_4 - T_3}{T_6 - T_3} \qquad\qquad 05$$

The simple GT cycle commonly has a higher turbine exit temperature than exit temperature of the compressor as shown through T-s diagram in Fig. 7. There is a chance to use turbine exhaust gases which preheat the air between the compressor and the combustion chamber, this process is known as regenerative process. It is also noted that if the pressure ratio of the compressor is large enough, then the compressor release temperature will be high and turbine exit temperature will be low, it requires no heat exchanger. The net workout is unaffected by the addition of a heat exchanger. The heat provided to the system reduces and remaining heat is taken by exhaust heat.

Thus cycle efficiency becomes

$$\eta = \frac{\text{net work output}}{\text{heat supplied}} = \frac{C_p(T_3 - T_4) - C_p(T_2 - T_1)}{C_p(T_3 - T_5)} \qquad\qquad 06$$

The specific fuel consumption in this proper term to express real cycle performance, i.e. fuel mass flow per unit power output. To obtain this, the fuel/air ratio must be found. In the course of calculating the net output per unit mass flow of air, the temperature at inlet to the combustion chamber (T_4) will have been obtained; and the temperature at outlet (T_5), which is the maximum cycle temperature, will normally be specified. The problem is therefore to calculate the fuel/air

13

ratio f required to transform unit mass of air at T_4 and f kg of fuel at the fuel temperature t_f to (1 +f) kg of products at T_5.

$$\sum (m_i h_{i5}) - (h_4 - fh_f) = 0$$
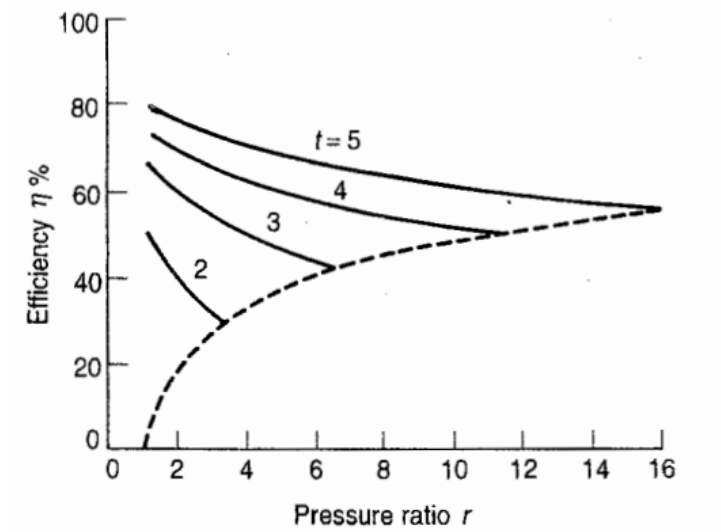
Figure 10. Efficiency vs Pressure Ration for recuperated engine

where m_i is the mass of product i per unit mass of air and h_i is its specific enthalpy. Making use of the enthalpy of reaction at a reference temperature of 25 °C, ΔH_{25}, the equation can be expanded in the usual way [5] to become

$$(1+f)c_{pg}(T_5\text{-}298)+f\Delta H_{25}+ c_{pa}(298\text{- }T_4)+fc_{pf}(298\text{- }T_f)=0$$

where c_{pg} is the mean specific heat of the products over the temperature range 298 K to T_5. ΔH_{25} should be the enthalpy of reaction per unit mass of fuel with the H_2O in the products in the vapor phase, because T_5 is high and above the dew point.

Abovementioned parameters have been calculated on the assumption that the fuel is completely burnt. The most appropriate method of allowing for combustion loss is by introducing a *combustion efficiency* defined by

$$\eta_b = \frac{\text{theoritical f for given } \Delta T}{\text{actual f for given } \Delta T}$$

Once the fuel/air ratio is known, the fuel consumption m_f is simply f x m where m is the air mass flow, and the specific fuel consumption can be found directly from

14

$$SFC = \frac{f}{PW_{shaft}} \qquad\qquad 07$$

$$PW_{shaft} = PW_{shaft\_t} - PW_{shaft\_c} \qquad\qquad 08$$

$$\eta_{cycle} = \frac{3600}{SFC * Q_{net}} \qquad\qquad 09$$

2.3. Challenges in Implementation of MGT in Automobiles

Micro Gas Turbine (MGT) are a relatively new type of combustion turbines that can produces both heat and electricity on a small scale. MGT offers an efficient solution to stand alone electricity generation system. This report focuses on the development of a micro gas turbine driven by compressed methane gas. Small turbines have always been efficient and powerful. Moreover, they are ideal to produce thrust, but ground vehicles operate using torque rather than thrust producing a whole host of engineering challenges. The revolution in electric vehicles has bypassed a large number of these issues because the turbine can be used to recharge a battery rather than directly power the car [6]. It is only because of these new Engineering techniques and technologies that electric vehicles might have MGT as standard features soon.

Besides its development and establishment, these machines are still facing implementation challenges due to turbomachinery design issues, cost minimization and combustion management.

References

[1] Thermodynamics – An Engineering Approach by: Cengel & Boles. Chapter 09 "Gas Power Cycles"
[2] Microturbines: Application for Distributed Energy Systems by By Claire Soares.
[3] Balje (1981) Turbomachines - A Guide to Design, Selection, and Theory
[4] Gas Turbine Theory by Rogers and Cohen. Chapter 2 "Shaft power cycles"
[5] ROGERS, G. F. C. and MAYHEW, Y. R. Engineering Thermodynamics, Work and Heat Transfer, 5th edition (Longman, 1994).
[6] Microturbines: Application for Distributed Energy Systems by By Claire Soares

Chapter 3

ELECTRICAL SIDE CALCULATIONS

As one single cell cannot meet power and driving range requirement in an electric vehicle. This is needed to construct battery packs with hundreds of single cells connected in parallel and series. The most important difference between a single cell and a battery pack is cell variation. Not only does cell variation effects pack energy density and power density, but also it causes early fade of battery packs and even results in safety issues.

The commercialization of pure electric vehicles requires a certain mileage, long life and high security. Hence, a lot of studies have primarily focused on the single cell and new materials [1-4], in order to improve the energy density, power density and cycle life of the single cell. However, one single cell is unable to meet the power and energy requirements for electric vehicles. Hundreds of the single cells need to be connected in series and parallel together to construct battery packs [5-8] so as to provide enough power and energy to for electric vehicles to meet the requirements of its accelerated climbing and mileage. Unfortunately, due to the inconsistency of the manufacturing process and use of the process environment, the cell variation always exists [9-11] and are incapable to remove.

3.1. Battery Bank Modeling and Sizing

With the rapid development of electric vehicles, lithium-ion batteries are increasingly being used in automotive energy source. The bottleneck of these vehicles lies in the low energy density, high costs, and limited lifetime of the battery cells contained in a high-voltage battery pack. As the battery pack is a complex system that consists of various components, an efficient design is crucial for the success of electric vehicles [12].

Battery bank calculation needs charging time analogy which has been established prior to optimize battery bank model.

3.1.1. Charging Time Analogy

Charging time analogy estimation is ordinarily known as one of the key functions in battery bank management system for lithium-ion batteries in EVs. Though every effort is made for various online state of charge (SOC) estimation methods to reliably increase the estimation accuracy as much as possible within the limited on-chip resources, ref. [13] discusses the error sources for those SOC estimation methods.
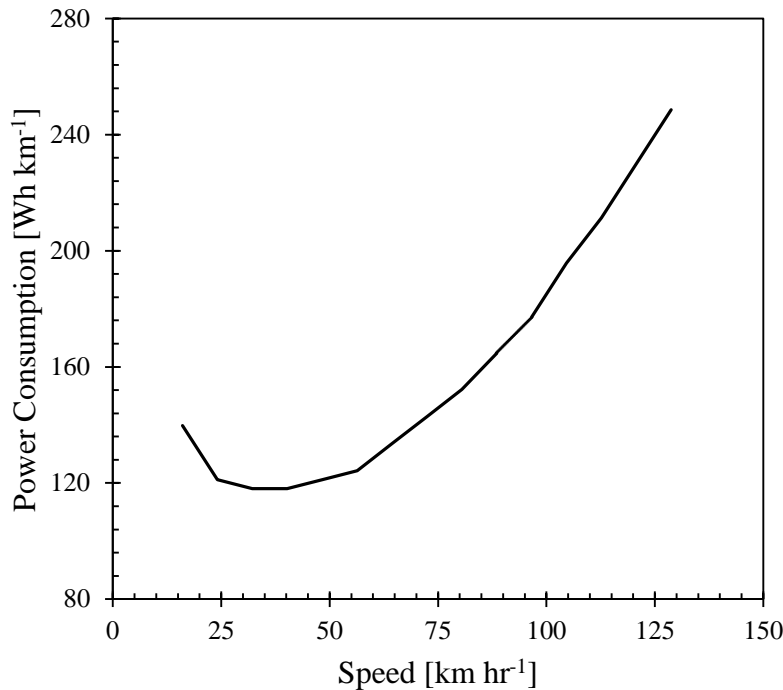
Figure 11. Power consumption vs speed chart redrawn from Tesla Motors data [14]

Charging analogy has been calculated to identify charging time with respect to average driving speed and power consumption. These analogies have been calculated according to power consumption behavior of tesla car given by Tesla Motors [14]. Vehicle speed vs. power consumption profile at different speeds of Tesla Model S P85 is redrawn in Fig. 11. The figure illustrates that initially power consumption decreases from 10 - 40 km hr^{-1}. Beyond that, power consumption is increasing. By considering all these fluctuations in power consumption and other important parameters according to driving requirements, a series of calculation has been organized which can fulfil charging time analogy is shown in Fig. 12.
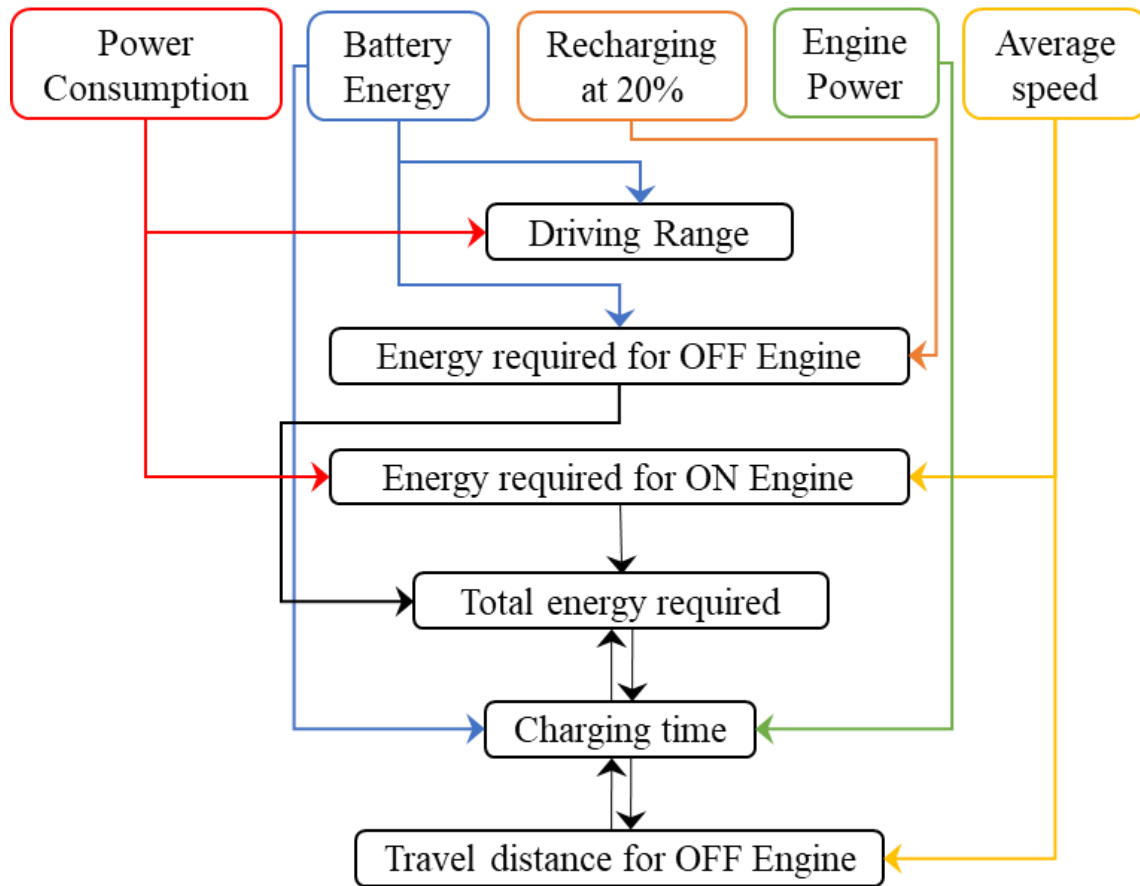
Figure 12 . Charging time analogy process

Detailed analysis for driving range and charging time is given in this study. Driving ranges R are calculated for different battery sizes (20 to 25 kWh) for the identification of their performances by considering different power consumption (P_c) withdrawn from respective batteries E_b, which is given as:

$$R = E_b \times P_b \qquad\qquad 10$$

Charging time analogies and driving ranges may be represented in tabular form as given in table 1. This reference table is representing all calculations at different driving speeds ranging from 60 - 120 km hr^{-1}. These speeds are based on typical traffic scenarios in countries. People in the cities usually drive under 50 km hr^{-1}. On national highways the average driving speed is noted around 80-100 km hr^{-1}, whereas on the motorways, the average speed of the car is 120 km hr^{-1}.

In order to analyze driving range with respect to speed variation, power consumption at different speeds (60 - 120 km hr^{-1}) are calculated. This range has been considered to facilitate city as well

as highway traveling to maintain driving range around 100 kilometers with 20-25 kWh battery pack. It has been noted that by adding all the driving variation, smaller battery bank such as 20 kWh is not suitable to avail an average driving range of 100 km. Hence, all similar calculations were done for 22-24 kWh which proves that average driving range of 100 km is available by means of 22 kWh battery bank size. Driving range vs speed profile as shown in Fig. 13 has been established on different battery energies from 20-25 kWh and this hypothetical case requirement is being fulfilled by 22 kWh battery bank. Figure 13 illustrates that the driving range is inversely proportional to the driving speed. Power consumption increases due to increase in speed, resulting in escalation of discharge rate and consequently decreasing the overall driving range.
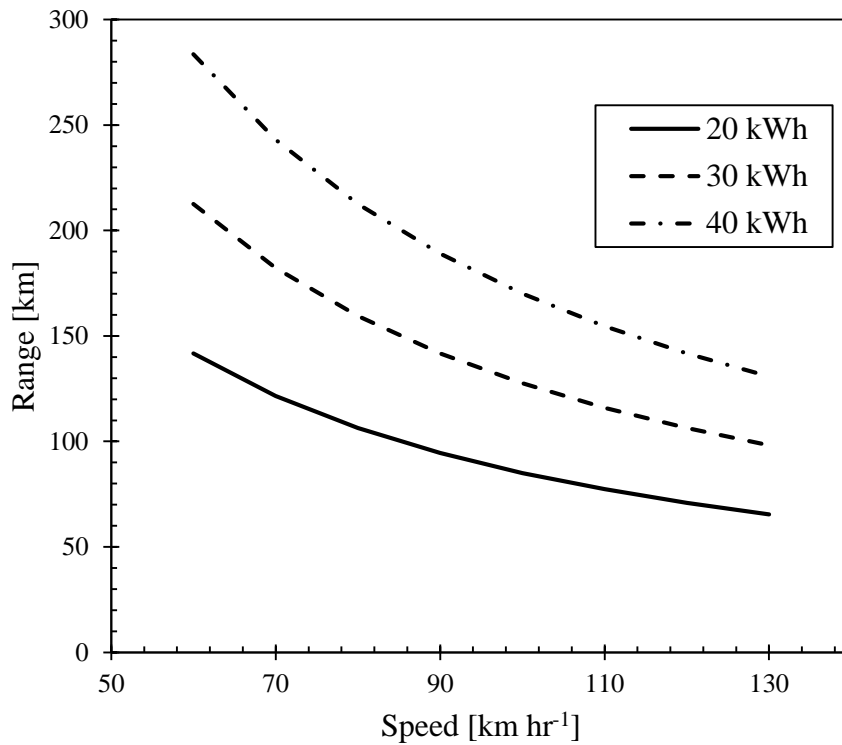
Figure 13. Range vs Speed Chart calculated on different battery energies

Charging time analogy calculations with input parameters such as power consumption P_c, battery energy storage capacity E_b, engine power P_e, point of recharging SOC_r and average speed s are being prepared using the following set of equations. Remaining energy after 80% drainage ($E_{20\%}$) is calculated as:

$$E_{20\%} = E_b \times 20\% \hspace{3cm} 11$$

Battery bank will give power to the electric motor until battery is drained by 80% of its capacity which is also called as SOC_r. The time taken to recharge the battery bank depends upon battery capacity E_b and engine power P, which is calculated as:

$$t_{ON,engine} = \frac{E_b}{P_e} \qquad\qquad 12$$

After drainage of battery up to 80%, the range extender MGT would begin operation to recharge the batteries without stopping the vehicle. This distance will be dependent upon car average speed and the time which it takes for travelling and is given as:

$$d_{ON,engine} = t_{ON,engine} \times s \qquad\qquad 13$$

Energy required for ON engine ($E_{ON,engine}$) is calculated with the help of distance covered by vehicle ($d_{ON,engine}$) as:

$$E_{ON,engine} = P_c \times d_{ON,engine} \qquad\qquad 14$$

Total energy required ON Engine (E_t) mode is dependent upon energy consumed by EV during ON engine mode and the energy required for battery recharging from SOC 20% to 100% (E_r). It is estimated as:

$$E_t = E_r + E_{ON,engine} \qquad\qquad 15$$

Total time of charging t_t is estimated to be:

$$t_t = \frac{E_t}{P} \qquad\qquad 16$$

Travel distance for OFF engine is actual driving range of electric vehicle before engine restarts is finally calculated as:

$$d_{OFF,engine} = R \times 0.8 \qquad\qquad 17$$

Similarly, the time taken to for battery bank deplete to this level ($SOC_{20\%}$) when engine restarts is calculated as:

$$t_{OFF,engine} = \frac{s}{d_{OFF,engine}} \qquad\qquad 18$$
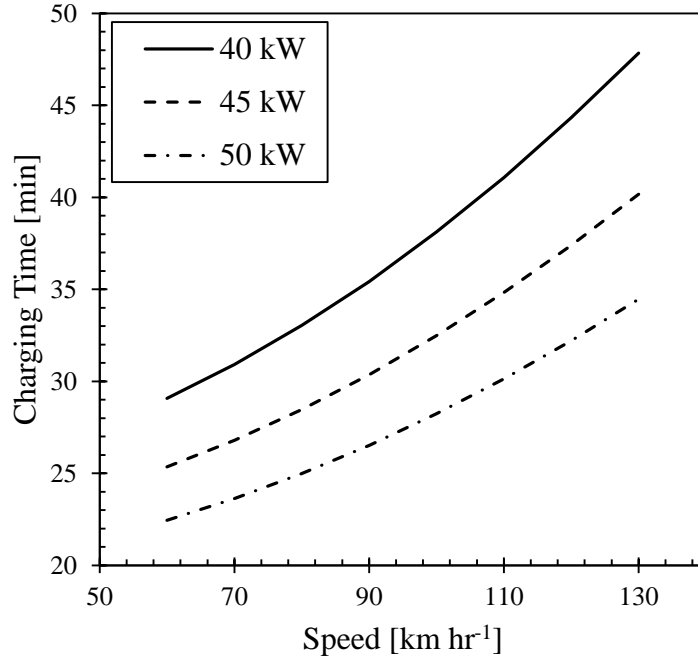
Figure 14. Charging Time vs Speed chart calculated on different speeds

Figure 14 illustrates the required charging time variation at vehicle speed. The curves have been constructed for different MGT sizes. The plot shows that with increase in the vehicle speed, the charging time increases due to depletion of battery bank charge. Moreover, a larger MGT compensates for the depletion in the battery charge by charging the bank faster than the smaller equivalents. MGT modeling will be discussed in detail later in this study where different sized of MGT is analyzed for optimum efficiency.

3.1.2. Battery Bank Model

With an aim to minimize the size of the battery pack to achieve a 100 km driving range, following set of equations defined in ref. [15-17] have been used. Battery energy is calculated as:

$$E_c = Q_c \times V_d \qquad 19$$

Where Q_c is cell capacity and V_d is cell voltage. This calculation is followed by energy density E_d and charge current I_c for one cell with the help of cell dimension (volume V_c) and its charge rate (c_r).

$$E_d = \frac{E_c}{v_c} \qquad 20$$

$$I_c = Q_c \times c_r \qquad 21$$

Time of charging t is calculated by considering I_b dependence over Q_c as:

21

$$t = \frac{I_c}{Q_c} \qquad \qquad 22$$

Abovementioned cell calculations are used to estimate voltage V_b and current I_b of battery bank.

$$V_b = N_c \times V_d \qquad \qquad 23$$

$$I_b = I_c \times N_s \qquad \qquad 24$$

Figure 15. Battery weight vs Energy chart representing increment in energy causes increase in weight

Where N_c and N_s are number of cell and number of series respectively. Similar to single cell's capacity, battery bank capacity is also calculated with the help of I_b and t:

$$Q_b = I_b \times t \qquad\qquad 25$$

Energy of battery bank E_b is final outcome of battery bank model which is calculated as:

$$E_b = Q_b \times V_b \qquad\qquad 26$$

For the calculation of battery pack weight, total number of cells are calculated with series data.

$$N_t = N_c \times N_s \qquad\qquad 27$$

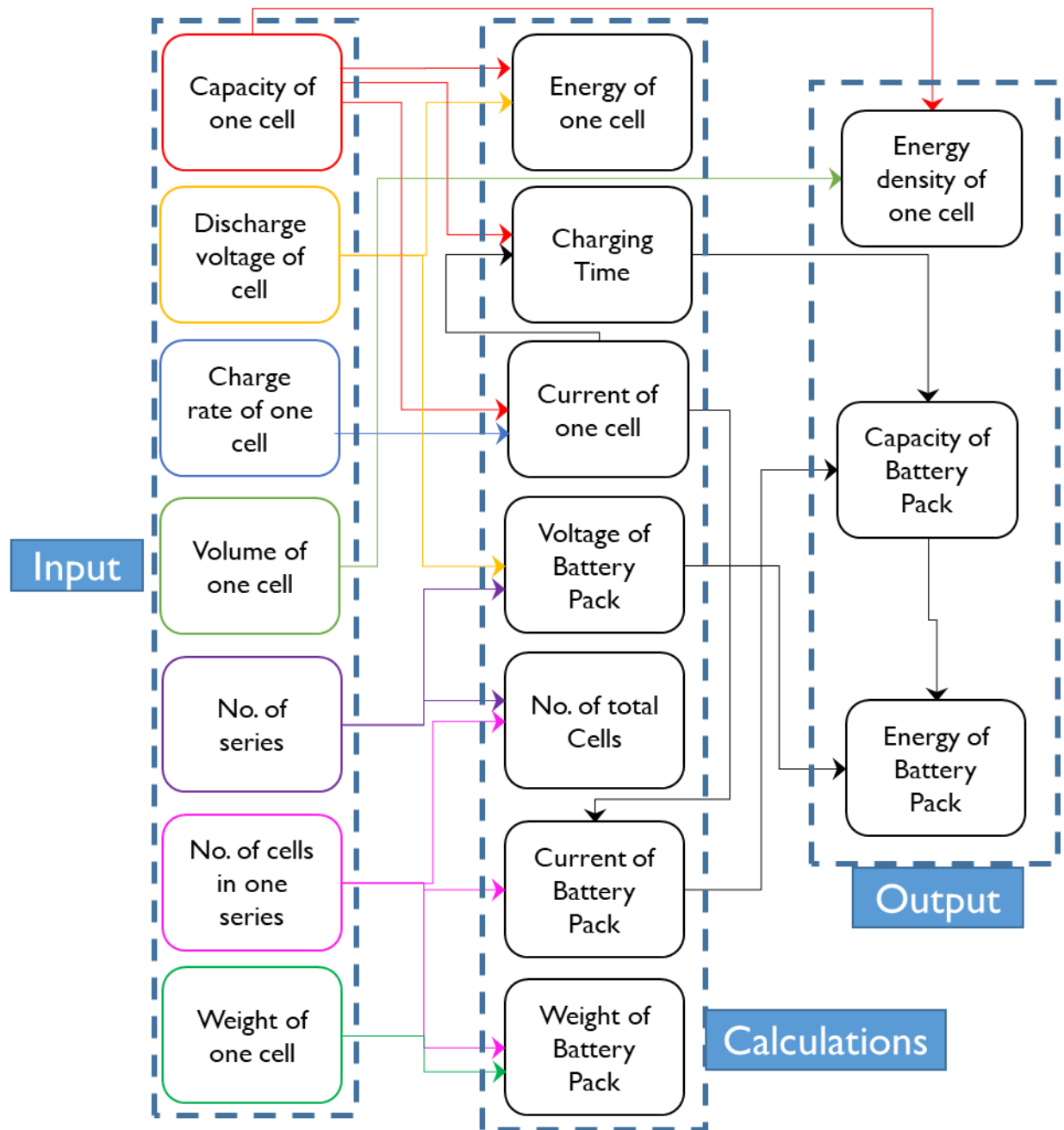Thus, battery bank weight is estimated as:

$$w_b = w_c \times N_c \qquad\qquad 28$$

In EVs, batteries are packed in small metal boxes. On an average, weight of battery pack w_p is 1.47 (packing factor) times weight of battery bank.

$$w_p = w_b \times 1.47 \qquad\qquad 29$$

Figure 15 illustrates the calculation sequence in detail.

3.1.3. Results and Discussion

From these equations, battery pack calculations are made for different energy storage capacities. Figure 15 shows calculation sequence for battery bank modeling and its calculation can be seen in Table 2. It shows various batteries with respect to different energy storage capacities and battery bank weights. Increasing energy causes increment in weight of battery pack. Minimum possible battery pack is desired to achieve daily running to reduce the cost of the EV. Figure 16 shows that the battery pack weight increases with increasing energy storage capacity due to much larger number of cells. Note that for the Tesla Model S P85 baseline EV, a battery bank size in the range of 20-25 kWh is selected based on the charging time analogy elaborated in the previous section of the paper.

Panasonic has developed high capacity Lithium Ion Battery Cells [18]. These cells are being used in EVs [19-20] and have been recommended in this study. Table 2 shows specification of one cell as well as combination of battery bank. This cell particularly, NCR18065A, has capacity and

Description	Specification					
Capacity of one cell, Q_c [Ah]	4	4	4	4	4	4
Avg. Discharge Voltage of one cell, V_d [V]	3.4	3.4	3.4	3.4	3.4	3.4
Energy of one cell, E_c [Wh]	13.6	13.6	13.6	13.6	13.6	13.6
Height of cell, h_c [mm]	64.93	64.93	64.93	64.93	64.93	64.93
Diameter of cell, d_c [mm]	18.2	18.2	18.2	18.2	18.2	18.2
Volume of one cell, v_c [mm3]	16894.07	16894.07	16894.07	16894.07	16894.07	16894.07
Volume of one cell, v_c [L]	0.02	0.02	0.02	0.02	0.02	0.02
Energy Density of one cell, E_d [Wh L-1]	805.02	805.02	805.02	805.02	805.02	805.02
Charge Rate, c_r [cr]	2	3	4	2	3	4
Current of one cell, I_c [A]	8	12	16	8	12	16
Time of charging, t [hr]	0.5	0.333333	0.25	0.5	0.333333	0.25
Time of charging, t [min]	30	20	15	30	20	15
Number of cells in series, N_c [cells]	94	94	94	94	94	94
Number of series in parallel, N_s [series]	17	17	17	18	18	18
Number of total cells, N_t [cells]	1598	1598	1598	1692	1692	1692
Voltage of battery pack, V_b [V]	319.6	319.6	319.6	319.6	319.6	319.6
Current of the battery pack. I_b [A]	136	204	272	144	216	288
Capacity of battery pack, Q_b [Ah]	68	68	68	72	72	72
Energy of battery pack, E_b [kWh]	21.73	21.73	21.73	23.01	23.01	23.01
Weight of one cell, w_c [g]	54	54	54	54	54	54
Weight of batteries, w_b [kg]	86.3	86.3	86.3	91.4	91.4	91.4
Weight of battery pack, w_p [kg]	126.8	126.8	126.8	134.3	134.3	134.3

Table 1. Battery bank calculation

discharge voltage of 4 Ah and 3.4 Volts respectively, as provided by manufacturer [21]. Considering its energy (13.6 Wh calculated) and volume, energy density is estimated around 800 Wh L^{-1}. These cells are recharged at the rate of 2. Current of one cell is 8 - 16 Ampere depending upon charge rate. Higher charge rate offers fast charging and higher density in battery packs. Commercialized cells are available at charge rate of 2 as of yet, however further urbanization can lead to compactness of battery bank and quick recharging. This combination is taking 15-30 minutes for recharging. Voltage of battery bank is dependent upon number of cells designed in

one series. While as current of this combination is effected by independent current of one cell and its charging ability. Similarly, overall capacity of combination is dependent upon number of series in battery bank. Selection of battery bank has been done by considering NCR cell having charge rate of 2 due to its availability in commercial markets. Hence, battery bank energy lies in between 22-23 kWh which is fulfilling an EV to be delivered 100 km driving range. Consequently, the battery pack should weigh about 130 kg, which is relatively a light weight solution compared to the large battery bank installed in the baseline EV.
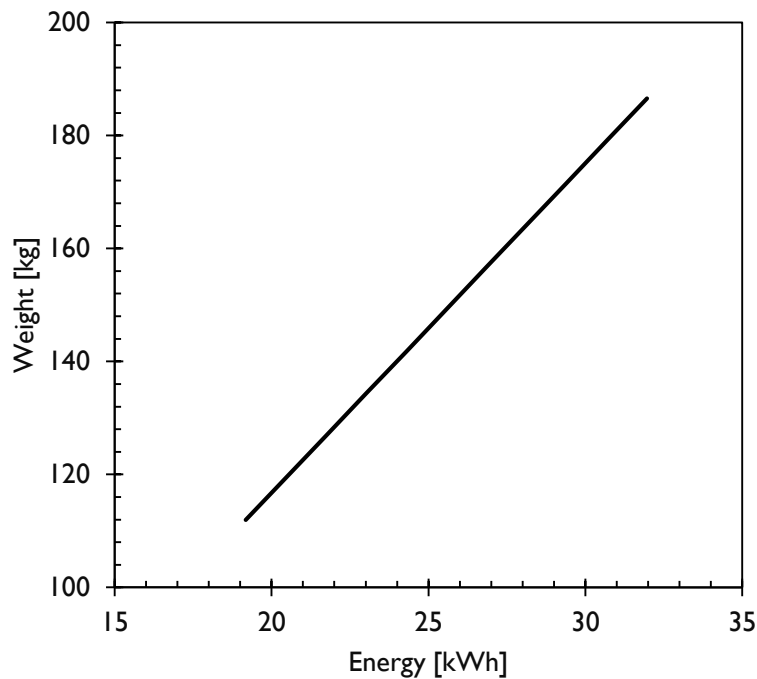
Figure 16. Battery weight vs Energy chart representing increment in energy causes increase in weight

Summary

In this chapter, we have studied battery bank calculations with engine compatibility for different sizes. These results were used to calculate charging time analogies for different size of batteries. It is concluded that, our hypothesis to recharge battery bank within 15-20 minute is wrong, however calculated charging time is coming out to be 30 minutes for 22 kWh batteries in order to have driving range of 100 km on average.

References

[1] Etacheri V, Marom R, Elazari R, et al. Challenges in the development of advanced Li-ion batteries: a review [J]. Energy & Environmental Science, 2011, 4(9):3243-3262

[2] Yuan L, Wang Z, Zhang W, et al. Development and challenges of LiFePO4 cathode material for lithium-ion batteries[J]. Energy & Environmental Science, 2011,4(2):269-284.

[3] Scrosati B, Hassoun J, Sun Y. Lithium-ion batteries. A look into the future[J]. Energy & Environmental Science, 2011,4(9):3287-3295.

[4] Jeong G, Kim Y, Kim H, et al. Prospective materials and applications for Li secondary batteries[J]. Energy & Environmental Science, 2011,4(6):1986-2002.

[5] Zheng Y, Han X, Lu L, et al. Lithium ion battery pack power fade fault identification based on Shannon entropy in electric vehicles[J]. Journal of Power Sources, 2013,223(0):136-146.

[6] Zheng Y, Lu L, Han X, et al. LiFePO4 battery pack capacity estimation for electric vehicles based on charging cell voltage curve transformation[J]. Journal of Power Sources, 2013,226(0):33-41.

[7] Zheng Y, Ouyang M, Lu L, et al. Cell state-of-charge inconsistency estimation for LiFePO4 battery pack in hybrid electric vehicles using mean-difference model[J]. Applied Energy, 2013,111(0):571-580.

[8] Offer G J, Yufit V, Howey D A, et al. Module design and fault diagnosis in electric vehicle batteries[J]. Journal of Power Sources, 2012,206(0):383-392.

[9] Kenney B, Darcovich K, MacNeil D D, et al. Modelling the impact of variations in electrode manufacturing on lithium-ion battery modules[J]. Journal of Power Sources, 2012, 213:391-401.

[10] Dubarry M, Truchot C, Cugnet M, et al. Evaluation of commercial lithium-ion cells based on composite positive electrode for plug-in hybrid electric vehicle applications. Part I: Initial characterizations[J]. Journal of Power Sources, 2011,196(23):10328- 10335.

[11] Lu L, Han X, Li J, et al. A review on the key issues for lithium-ion battery management in electric vehicles[J]. Journal of Power Sources, 2013,226(0):272-288

[12] C.Linse, R.Kuhn. Design of high-voltage battery packs for electric vehicles. Advances in Battery Technologies for Electric Vehicles. Woodhead Publishing Series in Energy. 2015, Pages 245-263

[13] Yuejiu Zheng, Minggao Ouyang, Xuebing Han, Languang Lu, Jianqiu Li. Investigating the error sources of the online state of charge estimation methods for lithium-ion batteries in electric vehicles. Journal of Power Sources. Volume 377, 15 February 2018, Pages 161-188

[14] Article: "Model S Efficiency & Range" by Tesla Motors. Article available online. https://www.tesla.com/en_CA/blog/model-s-efficiency-and-range?redirect=no

[15] Article: "Model S Efficiency & Range" by Tesla Motors. Article available online. https://www.tesla.com/en_CA/blog/model-s-efficiency-and-range?redirect=no

[16] Advanced Batteries. Materials Science Aspects. Author: Robert A. Huggins.

[17] Electrical Engineering Series, "Lithium Batteries and Other Electrochemical Storage System" by "Christian Glaize and Sylvie Genies"

[18] Panasonic Global Headquarter News. Development of high capacity lithium ion batteries. Article Published Online. https://news.panasonic.com/global/press/data/en091225-3/en091225-3.html

[19] Tesla Model S update

http://www.roperld.com/science/ElectricCarsMusings.pdf

[20] Article published online. Automotive Magazine. 2013 Automobile of the year, Tesla Model S. by David Zenlea. https://www.automobilemag.com/news/2013-automobile-of-the-year-tesla-model-s/

[21] Panasonic Cell NCR18650A specification. https://na.industrial.panasonic.com/sites/default/pidsa/files/ncr18650a.pdf

Chapter 4

MGT CONCEPTUAL DESIGN

4.1. Introduction

This section comprises the actual design point study and structure of the basic model that GSP uses to calculate the points numerically for its modeling and simulation. In this hypothetical case, a 22 kWh battery pack is selected for driving a Hybrid Electric Vehicle over a range of 100 kilometers. For this purpose, a thermodynamic model of an MGT of 40-50 kW is required to charge 22 kWh battery pack within 30 minutes. As a reference model Capstone C30 is taken during this study [1, 2]. Ambient conditions are taken into account according to Pakistan's climate changes. Detailed modeling has been done by considering component efficiencies followed by cycle optimization. Therefore, it was compulsory to get as much data about the MGT as possible. Table 3 shows design data.

4.2. Assumptions for GSP Simulations

GSP is a software program which has its boundaries. Before conducting the calculations, some assumptions are needed. These assumptions will be studied later in this chapter. During performance analysis, Capstone C30 was considered as reference and was also used to establish values in the scaling relationships. The available data of C30 from official manufacturing data or other reliable technical sources was limited. These values were used for engine performance specifications where possible.

4.3. Conceptual Design

Micro gas turbine has been designed and simulated numerically in GSP followed by MS EXCEL in order to present results in multiple formats.

4.3.1. Design Point

Gas turbine performance means Design Point Performance, Off-Design Performance and Transient Performance. Design Point Performance is essential to the engine concept design

process. Off-Design Performance is the steady state performance of gas turbine as its operating condition is changed. Transient Performance deals with the operating regime, where engine performance parameters are changing with time. The design point is defined as running at the certain speed, mass flow and pressure ratio for which the components were designed. Variation of gas turbine performance over the complete range of power output is discussed in next chapter with the help of component performance evaluation [3, 4].

4.3.2. Modeling

Gas Turbine Simulation Program (GSP) version 17 was used for cycle modeling. Figure. 11 shows model diagram consisting of inlet, compressor, combustion chamber, recuperator and exhaust. A recuperator has been added to enhance the cycle efficiency. This MGT model has been modeled with design points which are discussed later in this study, and is used for conceptual design and component matching.
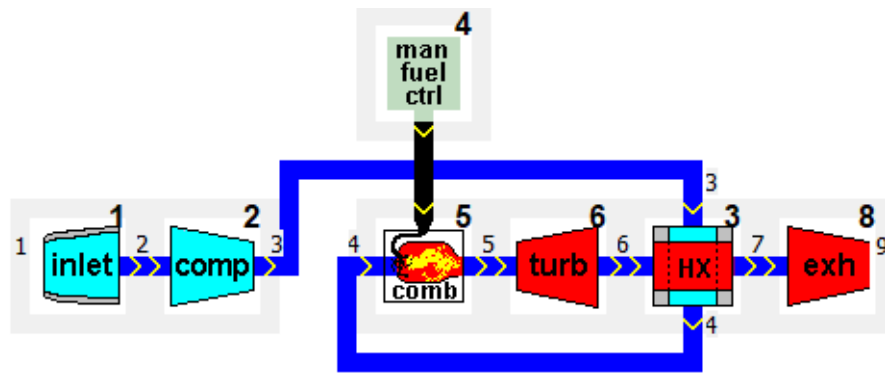
Figure 17. Conceptual design of MGT

MGT Design Parameters	
Static / Total Ambient Conditions	**Combustor**
Ambient Temperature = 315 K	Design combustion efficiency = 0.999
Ambient Pressure = 1.01325 bar	Design point rel. pressure loss = 0.02
Relative humidity = 67 %	Exit Temp = 1240 K
Inlet	**Turbine**
Design mass flow = 0.4 kg s^{-1}	Design rotor speed = 95000 rpm
Pressure Ratio = 1	Design efficiency = 0.82
	Expansion heat loss fraction = 0.5

Compressor

Design Rotor Speed = 95000 rpm   **Exhaust**

Design Efficiency = 75 %   Velocity coefficient CV = 1

Heat transfer fraction = 0.5   Thrust coefficient CX = 1

Pressure Ratio = 4   Throat CD = 1

Recuperator

Effectiveness = 0.9

Rel. total pressure loss:

Flow 1 = 0.015

Flow 2 = 0.04

Table 2. MGT Design Parameters for Gas Turbine Simulation Program

4.3.3. Study of thermodynamic cycle with GSP

Variables that were controlled during different series of simulations by the case control; Turbine Inlet Temperature (TIT) and compressor pressure ratio (PRc), turbomachinery component efficiencies (including turbine design efficiencies, compressor design efficiency and heat exchanger effectiveness) and air mass flow ($\dot{m}_a$) The generator efficiency most likely will vary slightly with scale but was assumed constant with limited error. The variables that were kept constant were combustion pressure drop and heat exchanger hot/cold side pressure loss.

Figure 18 describes output results of cycle performance study with carpet plot between SFC and Power. This carpet plot represents two different profiles which are compressor pressure ratio (PRc) and turbine inlet temperature (TIT). Both profiles show different behavior crating multiple intervals. These intervals demonstrate several engine data points. Moving from left to right, TIT increases which results in power rise and SFC fall. Hence it makes higher efficiency for engines. Due to metallurgical limitations, TIT cannot be increased beyond certain limits. Similarly, an increase in PRc vertically upward results in higher engine power allowing to an extent of SFC. Beyond this limit, SFC will be increased and engine power will remain constant which results in

decrease in overall efficiency. Carpet plot helped us to understand mutual correspondence in between engine power and SFC.

To achieve optimum efficiency from Fig. 18, a particular engine point is selected representing TIT and compressor pressure ratio as 1240K and 4 respectively. During this interval, the engine power coming out to be 47 kW and SFC to be 0.25 kg kWh^{-1}. Cycle Efficiency is calculated as 33.4%. This is optimum output from entire carpet plot giving maximum shaft power output.

4.4. MGT and Battery Pack matching

In addition to SFC and Shaft power from Fig. 18, battery energy compatible to respective engine power is shown in Fig. 19. which shows multiple intervals representing different engine power
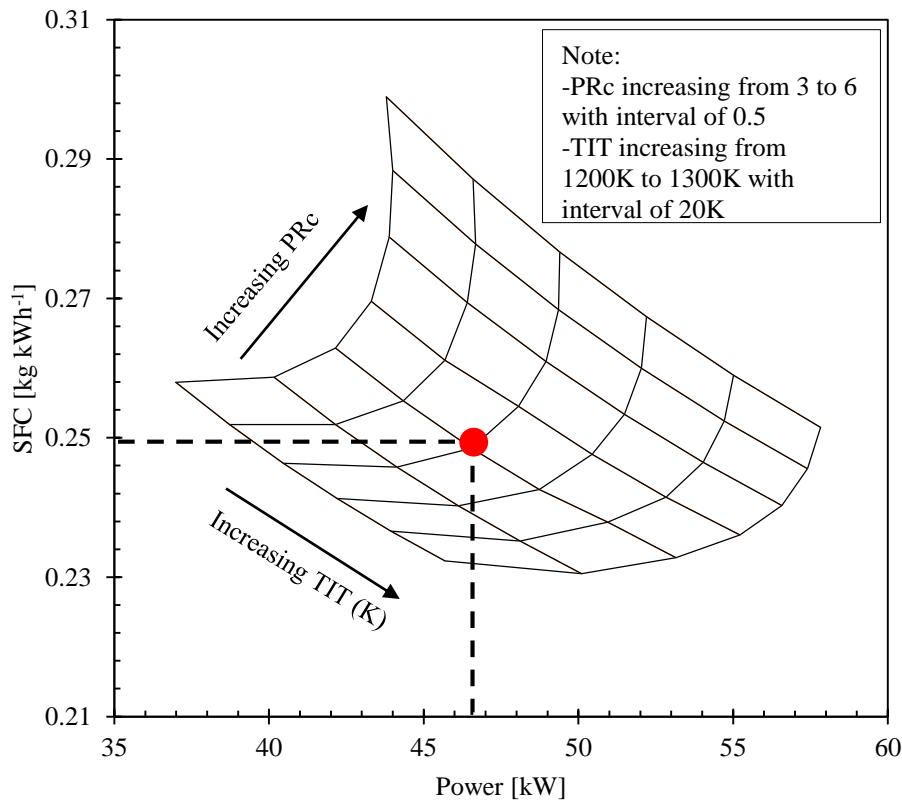
Figure 18. SFC vs Power chart with the help of output results from GSP

which can charge different battery packs in specific time. This is possible well-matched outcomes for both devices (MGT and Battery Pack). Each interval shows battery energy ranges from 16 kWh to 33 kWh and charging time from 22 to 36 minutes. Selected interval states 22 kWh battery energy. This study is further divided into two main categories depending upon battery energy and charging time requirement.

4.4.1. Analysis on constant Charging Time

A brief overview of battery energy vs power and their influence with TIT is given in Fig. 19a. All calculations are done on constant charging time in order to evaluate different battery energies developed by different engine power output. Engine shaft (Turbine output) power is mainly
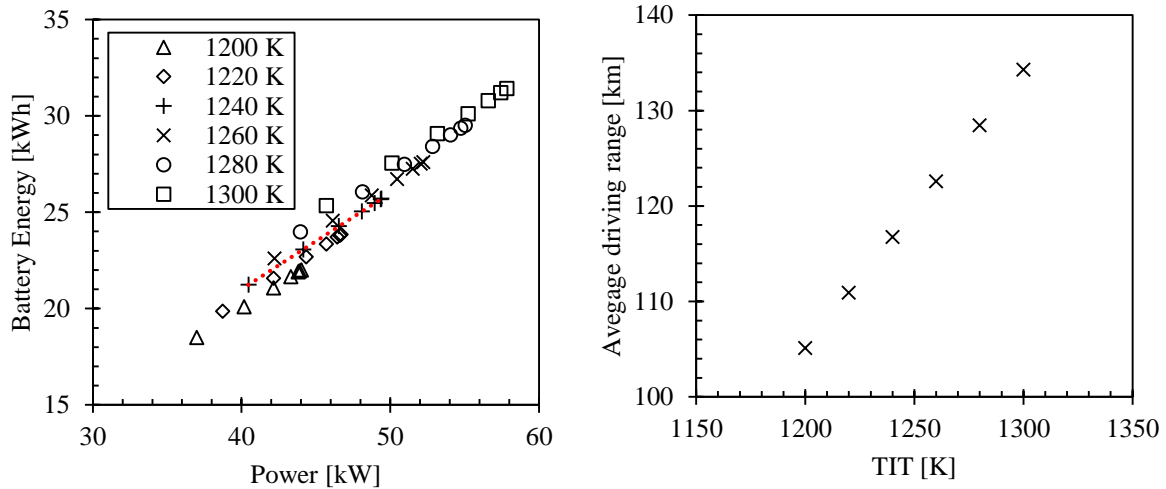

Figure 19. (a) Battery energy vs Power consumption on different TIT

(b) Average driving range vs TIT showing effect of higher TIT on driving range

dependent and directly proportional to TIT. Bigger engine helps to charge more batteries within the same time range. It helps to incorporate bigger battery pack to increase driving ranges of electric vehicles. Besides selection of 47 kW engine power as optimum output, various options are available on this data line. But due to machine design and metallurgical limitations, the temperature boundaries and SFC are noted to be increased beyond said values and efficiency to be decreased.

In Fig. 19a, temperature line is artificially elevated by 0.5 kWh to differentiate more clearly. It shows increment of battery energy due to increase in engine power. By choosing 1240K data line, it is noted that a range of engine power 40-50 kWh are available.

Figure 19b presents increment of turbine inlet temperature (TIT) to produce high shaft power which can develop more battery energy. High battery energy gives longer driving range.

4.4.2. Analysis on constant Battery Energy

This calculation has been done to illustrate charging time variation for different engines. Higher TIT influences turbine output which develops higher shaft power. Recharging of batteries is directly proportional to the power coming from MGT. Considering constant battery energy which
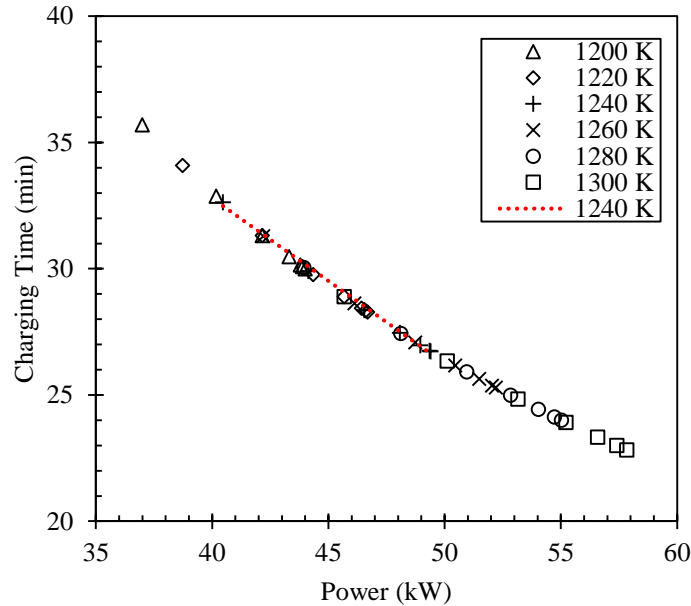

Figure 20. Charging Time vs Power on different TIT

leads to variation in charging time for different shaft powers. It clarifies charging time analogy dependence upon engine characteristics which is mainly dependent on TIT. Detailed variants are given in Fig. 20 in which battery energy is kept 22 kWh as constant. This gives numerous charging time on different TIT varying from 1200 to 1300 K.

Summary

An initial design model was built to generate conceptual design of MGT depending upon the various TITs and PRcs to observe different outcomes of GSP model. The input data of Capstone C30 obtained and optimized for national conditions and thesis requirement. A SFC vs Shaft Power analysis was conducted to determine the optimum design point for further simulations. These simulations are used to identify numerous behavior of MT with respect to component design efficiencies. Natural Gas was used in this examination. In order to make MGT technology more feasible, improvement towards cheaper materials for hot-end components such as the recuperator and turbine are necessary.

References

[1] The University of Queensland, Adam Head. June 2011 "Conceptual Design and Simulation of a Microturbine: An Electric Car Range Extender Application" Appendix A Capstone C30 Design Data.

[2] Capstone, C. (2009). Capstone Hybrid Vehicle Experience. California, USA, Capstone turbines

[3] ASME Proceedings, Power for Land, Sea and Air. Volume 1: Turbo Expo 2005, Reno, Nevada, USA, June 6–9, 2005, Kurzke, J. "How to create a performance model of a gas turbine from a limited amount of information."

http://proceedings.asmedigitalcollection.asme.org/proceeding.aspx?articleid=1584066

[4] Verbist, M. L. (2010). GSP Modeling Elements and Numerical Methods. Delft, TU Delft

Chapter 5

EVALUATION OF COMPONENT PERFORMANCE

This chapter aims to analyze engine performance and component characteristics of a micro gas turbine based on detailed measurement of various parameters. Another model to measure performance of a micro gas turbine was developed on GSP and performance parameters such as turbine exit temperature, exhaust gas temperature, engine inlet temperature, compressor discharge pressure and temperature, fuel and air flow rates were measured. The net gas turbine performance (power and efficiency based on the gas turbine shaft end) was isolated and analyzed. With the aid of measurement based simulation, component characteristic parameters such as turbine inlet temperature, compressor efficiency, turbine efficiency and recuperator effectiveness were estimated. Behaviors of the estimated characteristic parameters with operating condition change were examined and sensitivities of estimated parameters to the measured parameters were analyzed.

5.1. Turbine Design Efficiency

Overall efficiency of MGT is influenced with turbine design efficiency because it helps to extract more work output from the working fluid by changing geometrical parameters. Different simulations were run to check this feature and are graphically represented in Fig. 21 which represents carpet plots for turbine design efficiency. It shows variations in engine power and SFC for pressure ratio 3 to 6 and TIT from 1200 to 1300 K. Each carpet plot is built on different turbine design efficiency which are 75%, 80% and 85%. Higher turbine efficiency enhances its performance which increase in shaft power output and drops SFC.

5.1.1. Effect on constant Charging Time and Battery Energy

Figure 22a illustrates relation between battery pack energy and shaft power by keeping charging time constant. Higher turbine design efficiencies develop higher power. It is clearly seen that 75%
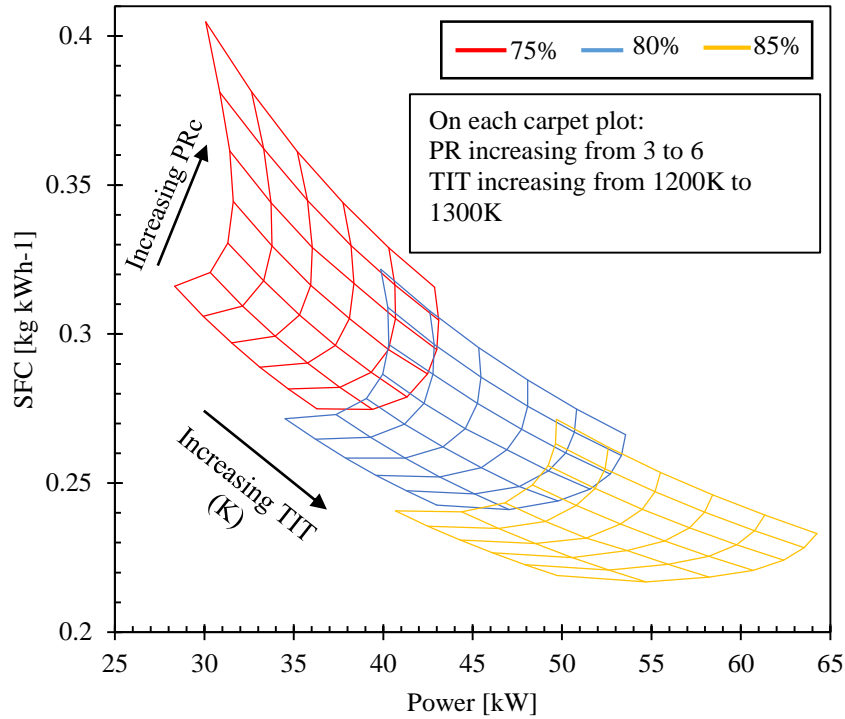
Figure 21. SFC vs Power on different Turbine Design Efficiency

efficiency of turbine is giving 26 kW shaft power whereas 85% efficiency is giving 65 kW output. Almost 1% improvement in design efficiency gives 3-4 kW power output. Similarly, battery pack energy is also dependent on turbine design efficiency. Since turbine design efficiency increases from 75% to 85%, battery energy rises from 15 to 33 kWh which results in longer driving ranges.
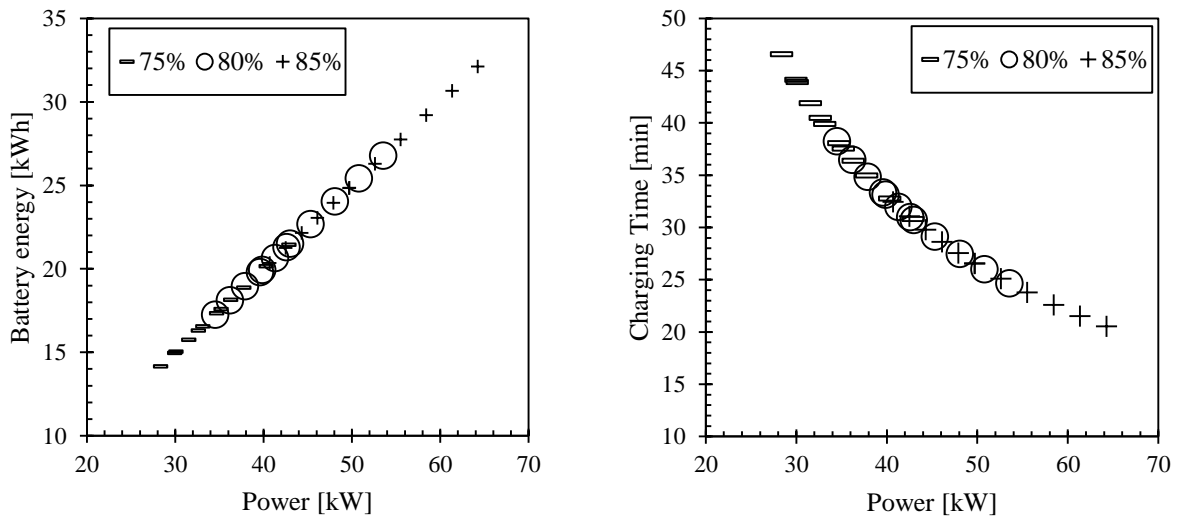

Figure 22. (a) Battery energy vs Power calculated on different turbine design efficiencies
(b) Charging Time vs Power on different Turbine Design Efficiency

Figure 22b describes variation in charging time due to increase in turbine design efficiency. In this case battery energy is kept constant at 22 kWh to identify charging time minimization. Efficient engine recharges battery packs in lesser time.

5.2. Heat Exchanger Effectiveness

Growing demand for environment friendly gas-turbine engines with lower emissions and improved specific fuel consumption can be met by incorporating heat exchangers into gas turbines. It is noted that SFC is decreased when heat exchanger effectiveness is increased. In a gas turbine engine, air is compressed, mixed with fuel, which is then burned and used to drive a turbine. The recuperator transfers some of the waste heat in the exhaust to the compressed air, thus preheating it before

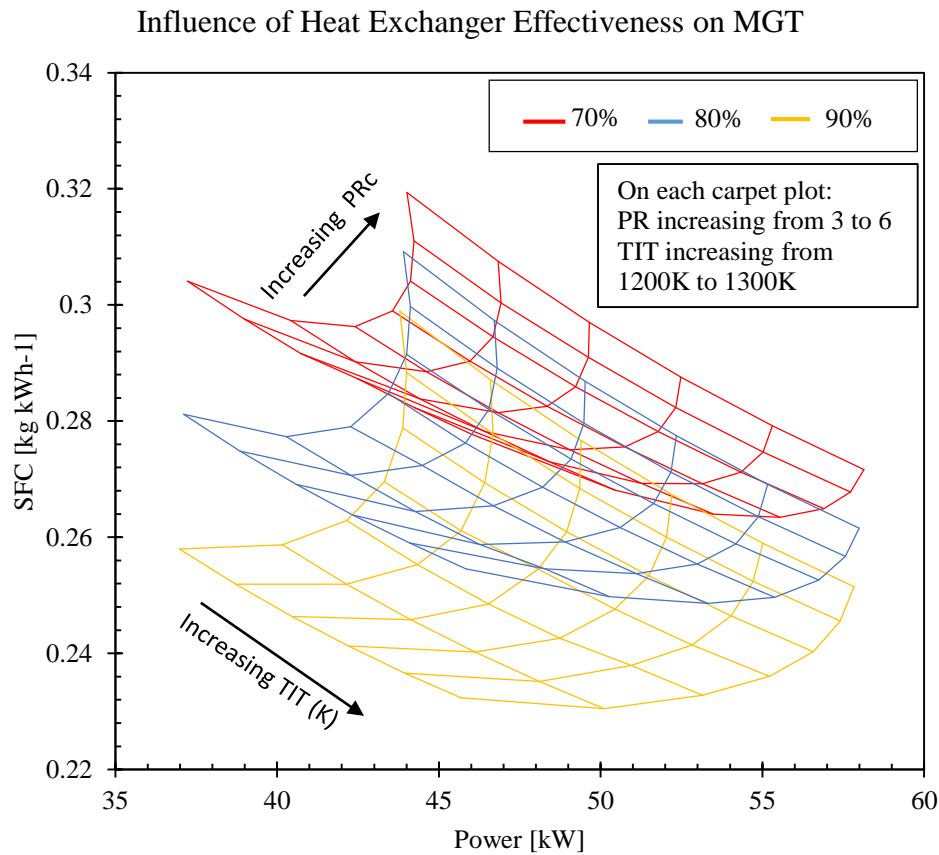Influence of Heat Exchanger Effectiveness on MGT

Figure 23. SFC vs Power on different HX effectiveness

entering the fuel burner stage. Since the gases have been pre-heated, less fuel is needed to heat the gases up to the turbine inlet temperature. By recovering some of the energy usually lost as waste heat, the recuperator can make a heat engine or gas turbine significantly more efficient. Figure 23

shows, as heat exchanger effectiveness is increased, SFC drops which increase overall efficiency. There is no influence of heat exchanger effectiveness on power, thus shaft power remains constant.

5.2.1. Effect on constant Charging Time and Battery Energy

Figure 24a presents heat exchanger effectiveness impact on battery energy vs shaft power and it is clearly seen that there is no change in output profile if heat exchanger effectiveness changes. Because recuperator doesn't change shaft power rather it only decreases SFC at the inlet of combustion chamber. As already discussed, recuperator helps to pre heat the incoming gases from compressor. Similar to shaft power, battery energy also remains constant as shown in Fig. 24b. It illustrates that increase in shaft power drops charging time but there is no change in output profile if heat exchanger effectiveness is changed from 70% to 90%. It only drops fuel consumption in combustion chamber.
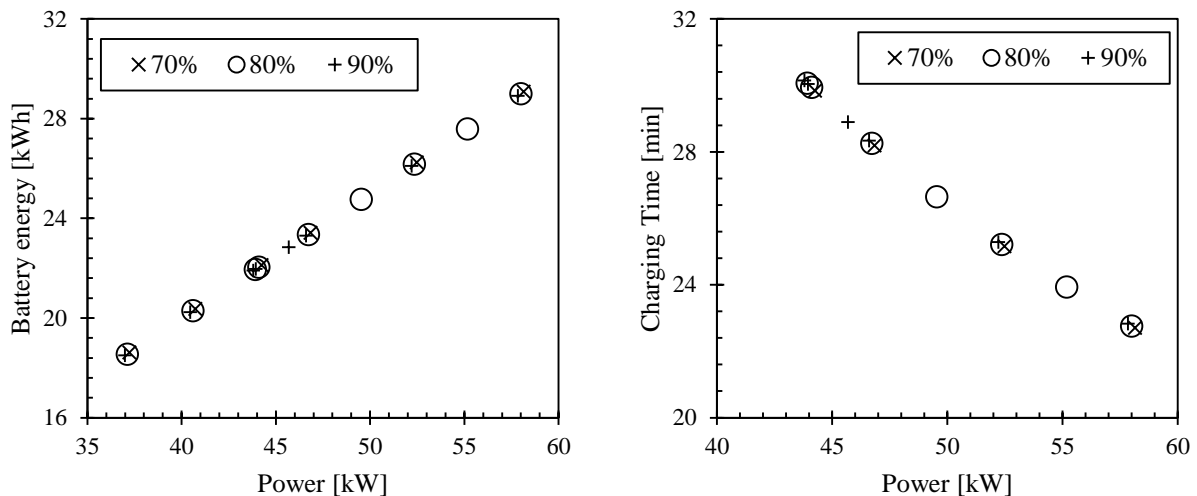

Figure 24. (a) Battery energy vs Power calculated on different HX efficiencies
(b) Charging Time vs Power calculated on different HX effectiveness

5.3. Compressor Design Efficiency

Similar to turbine design efficiency, compressor is a fundamental part of gas turbine technology and compressor design efficiency affect overall performance of gas turbine. Changes in compressor design efficiency cause changes in overall performance of MGT. A plot of specific fuel consumption versus shaft power is given in Fig. 25 where compressor design efficiency is changing from 60% to 80%. When compressor design efficiency is 60%, shaft power is around 15-30 kW and SFC is 0.35-0.85 kg/kWh. Increase in design efficiency is enhancing shaft power

37

and decreasing SFC which are 30-50 kW and 0.25-0.35 kg/kWh respectively. Further increased in design efficiency is helping combustion chamber to consume less fuel. Similarly, it helps turbine to expand more gases which increases shaft power output. 80% compressor design efficiency helps combustion chamber to consume less than 0.3 kg/kWh SFC and allows turbine to produce up to 65 kW energy.

5.3.1. Effect on constant Charging Time and Battery Energy

Compressor design efficiency impacts battery energy and charging time analogy. A plot of battery energy vs shaft power is given in Fig. 26a. In this calculation, charging time is kept constant. It
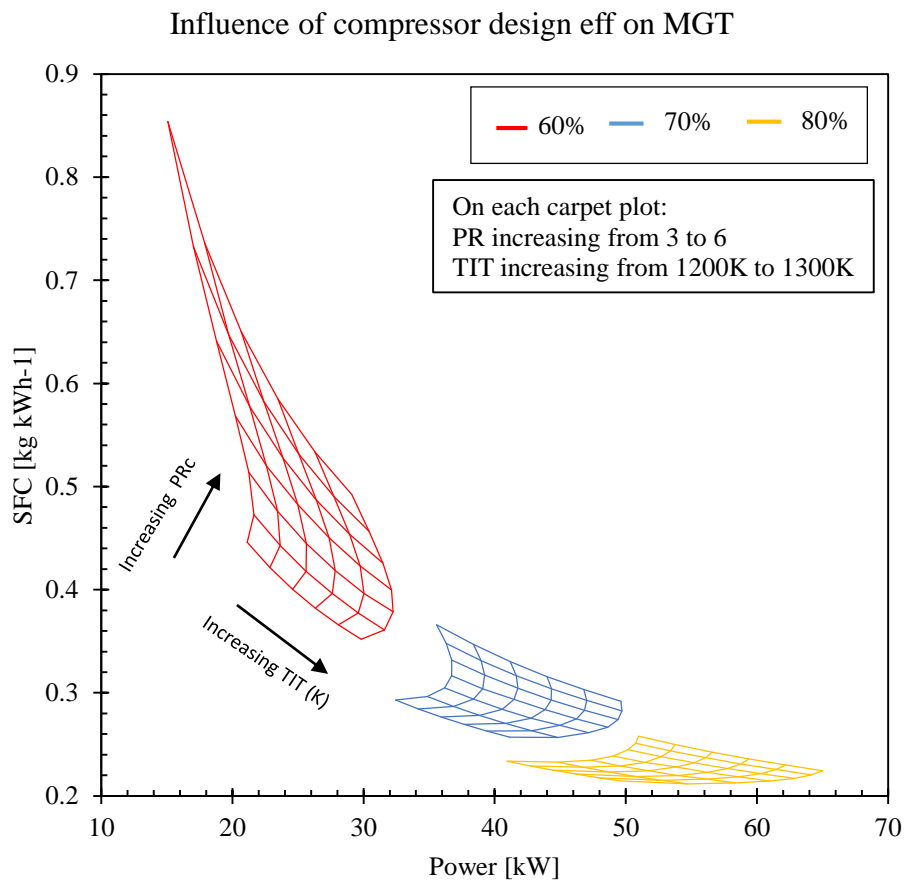

Figure 25. SFC vs Power on different compressor design

shows, through higher design efficiency, engine can recharge more batteries within specific time range. It develops longer driving ranges by these recharge battery packs.

Similarly, Fig. 26b illustrates variation of charging time on different shaft powers by keeping battery energy constant. It is shown that increase in compressor design efficiency decreases charging time to recharge same amount of battery pack.
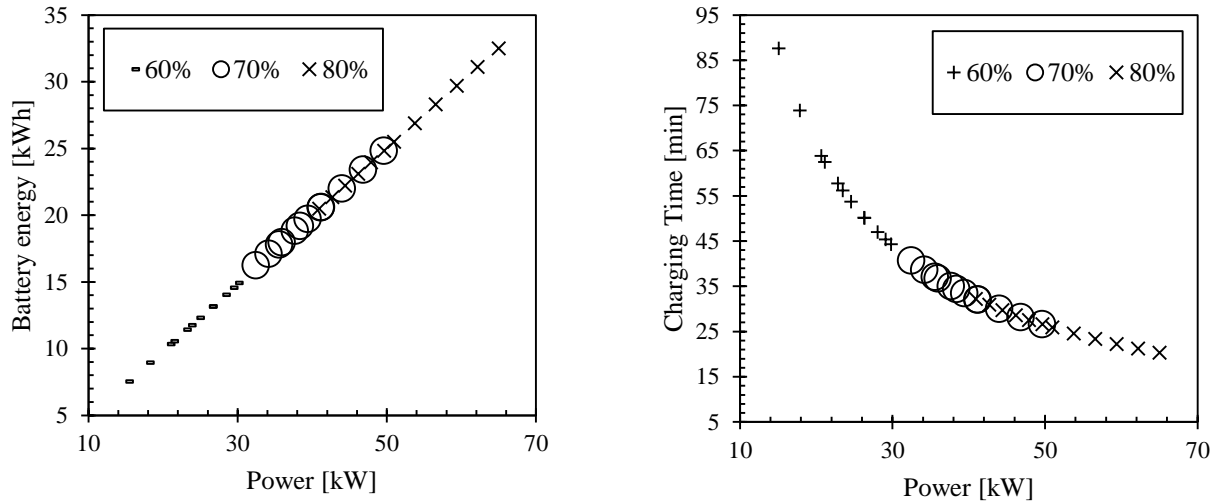
Figure 26. (a) Battery energy vs Power calculated on different compressor efficiencies
(b) Charging Time vs Power calculated on different compressor design efficiency

Summary

Component evaluation has been done in order to optimize cycle performance and to improvise micro gas turbine design performance. 3 techniques were used in this study. Enhancement of heat exchanger effectiveness, compressor design efficiency and turbine design efficiency. It is noted that shaft power output is not dependent on heat exchanger effectiveness. Whereas compressor deign and turbine design efficiency helps to increase output power of engine and can recharge battery pack in lesser time.

Chapter 6

MGT Experimental Setup

6.1. Introduction

Micro Gas Turbine (MGT) has been developed in Thermo Fluids Lab at Arizona State University by using off the shelf turbocharger. A turbocharger with the help of self-made combustion chamber is being converted into small scale gas turbine. Combustion chamber was added in between compressor and turbine section of turbocharger. This setup was solely built to run on gases as combustion fuel to evaluate combustion technique and synchronization between turbocharger and combustion chamber.
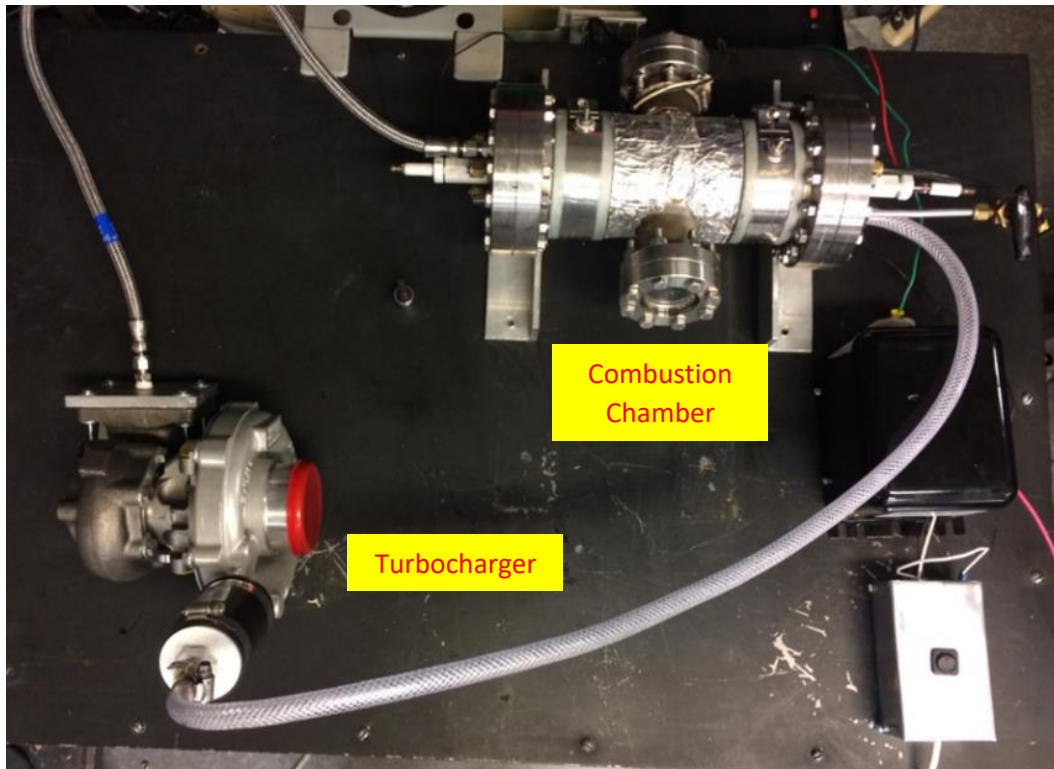
Figure 27. MGT Experimental Setup at ASU Lab

6.2. Experimental Procedure

MGT setup has been developed with the help of mainly two equipment as shown in fig:27.

1. Turbocharger
2. Combustion Chamber

Turbocharger and combustion chamber are two main components of in house MGT and its combination require further accessories which are given below;

1. Connections
    - Flanges
    - End Plate Fittings

2. Tubes / Fittings
    - Compressed Air Line
    - Fuel Line
    - Shop Air Line

3. Combustion Setup
    - Spark Ignition Setup
    - Remote Ignition
    - Gas Cylinder Fitting
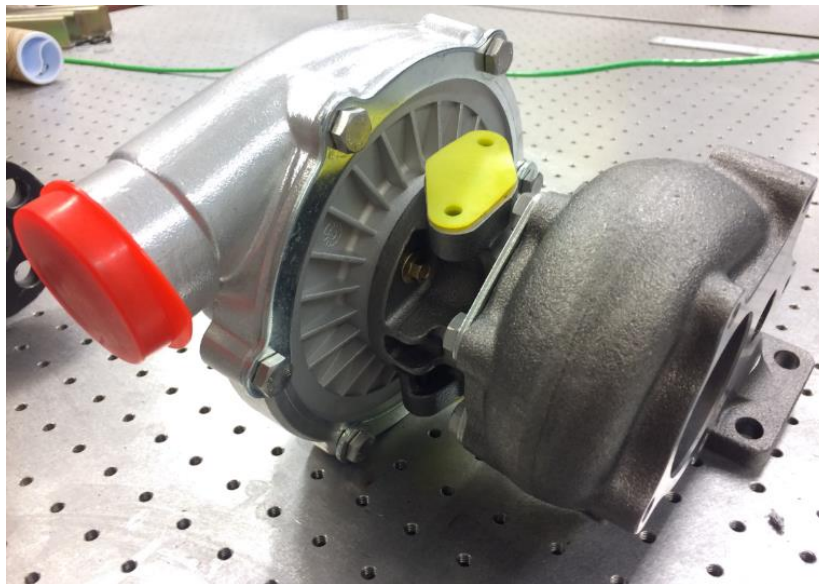
Figure 28: Turbocharger

Figure 29: Combustion Chamber

Combustion chamber which was built in the lab, was used to combust gaseous fuel which could be used to drive turbine part of turbocharger.
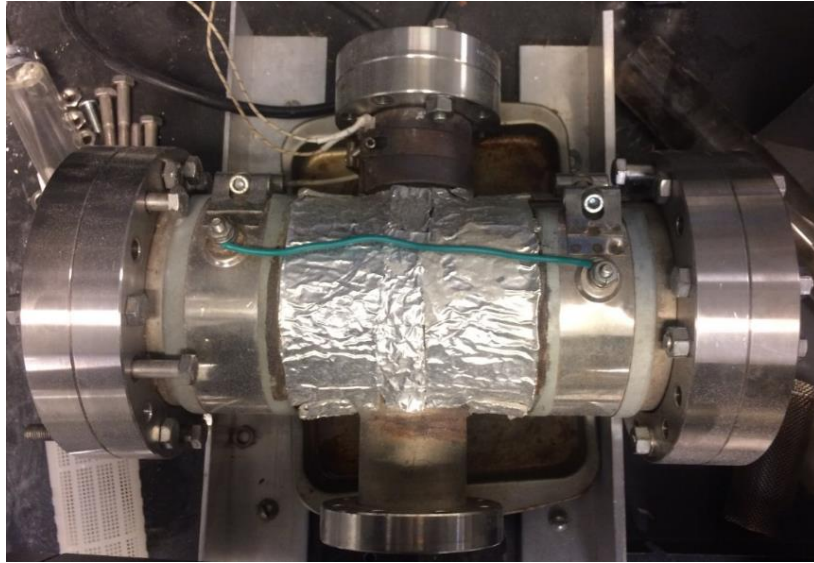

Figure 30: (a) Ignitor (b) Spark Probes

Spark ignition setup was built by using pulse generator to initiate spark in combustion chamber as shown in Fig. 30a. Figure 30b represents spark probes which are connected with ignitor to ignite combustion gases in chamber.

6.3. Working Principal

Initially turbocharger is manually cranked to obtain certain RPM on which it can automate combustion gases to drive turbine blade followed by compressor, that can compress air and push it into combustion chamber for further combustion.

Combustion is taken place by spark probes which are connected with ignitor to achieve sparks which help air fuel mixture to ignite in combustion chamber as shown in figure 31.
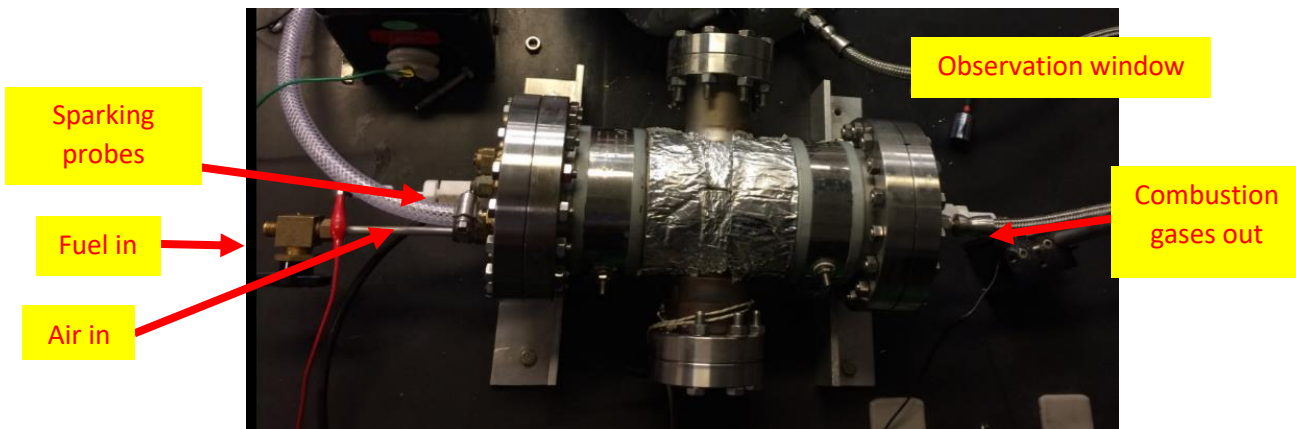
Figure 31. Combustion Chamber

High pressure and high temperature combustion gases travel to turbine section and transfer energy to turbine blades. Turbine is connected with compressor with the help of shaft which allows to rotate compressor on same RPM as Turbine as shown in figure 32.
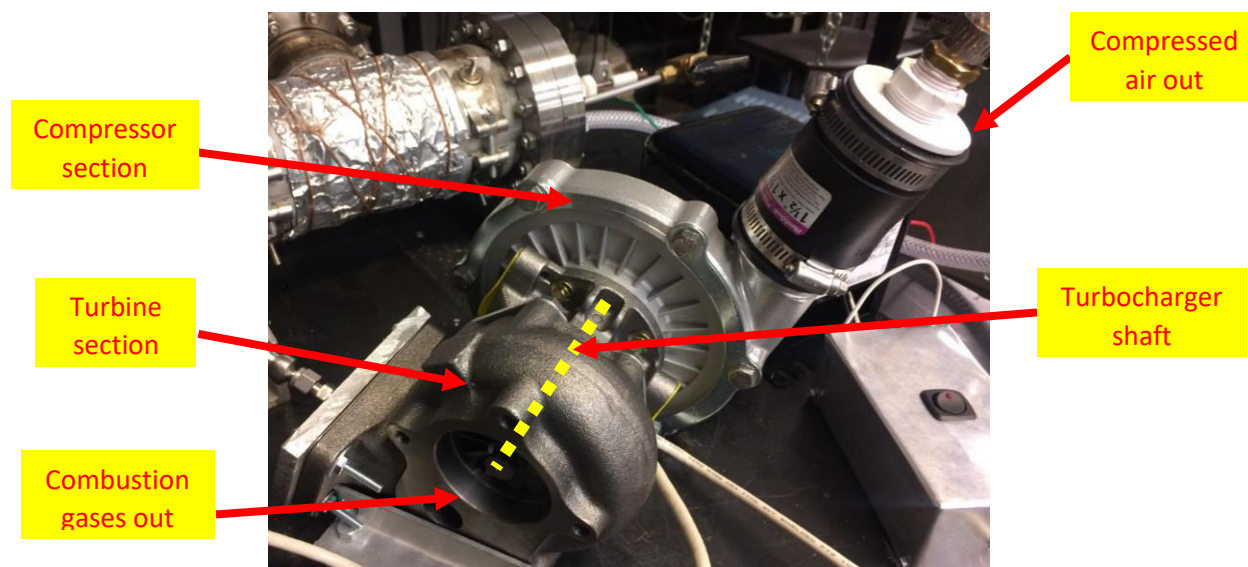
Figure 32. Turbocharger

This way cycle completes and it continues onwards.

Component testing was done on combustion chamber and turbine section to test them in isolation and measure their characteristics.

6.4. Observations

6.4.1. Combustion Chamber
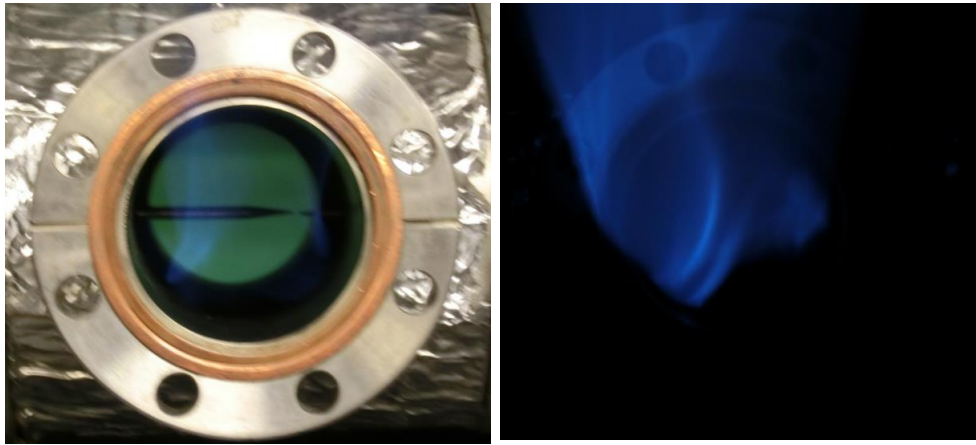
Figure 33: Combustion Tests

Combustion Chamber was tested by spark initiation with introduction of methane gas as shown in Fig. 33. While combustion was carried out, it was observed that combustion can be managed in a proper way by making fuel injection closer to spark as shown in Fig. 34.
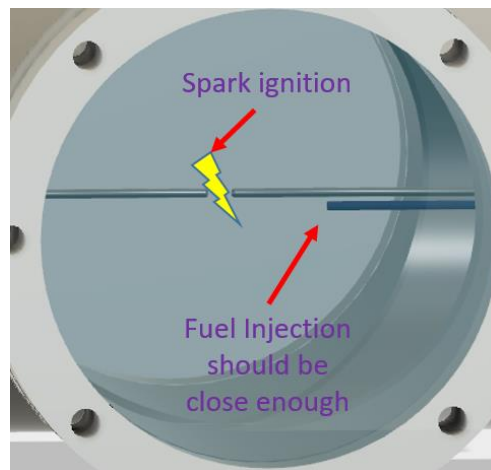
Figure 34: Fuel Injection approach

6.4.2. Turbine Section

Turbine section was tested to check its rotation on available pressure of shop air and managed to build flanges so that different readings can be measured on variable conditions.
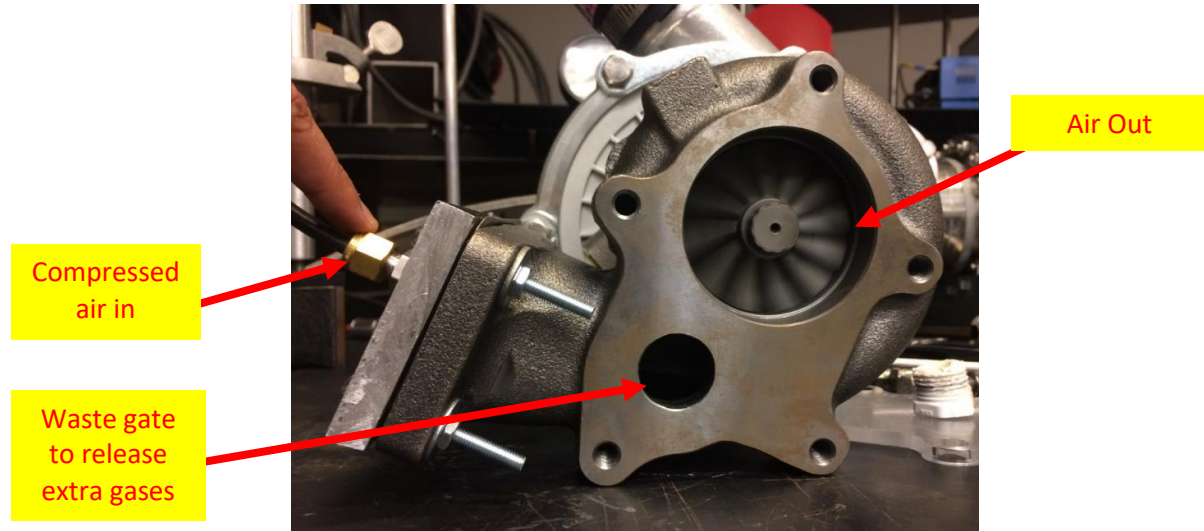
Figure 35. Side view of Turbocharger

Initially, shop air pressure was calculated as 98 Psi which was enough to rotate turbine wheel.

At the outer side of turbine, there is a waste gate which is used to bypass extra gas in order to limit RPM of turbine. In ideal case, it should remain close. Hence, in order to close waste gate, following observations were carried out.
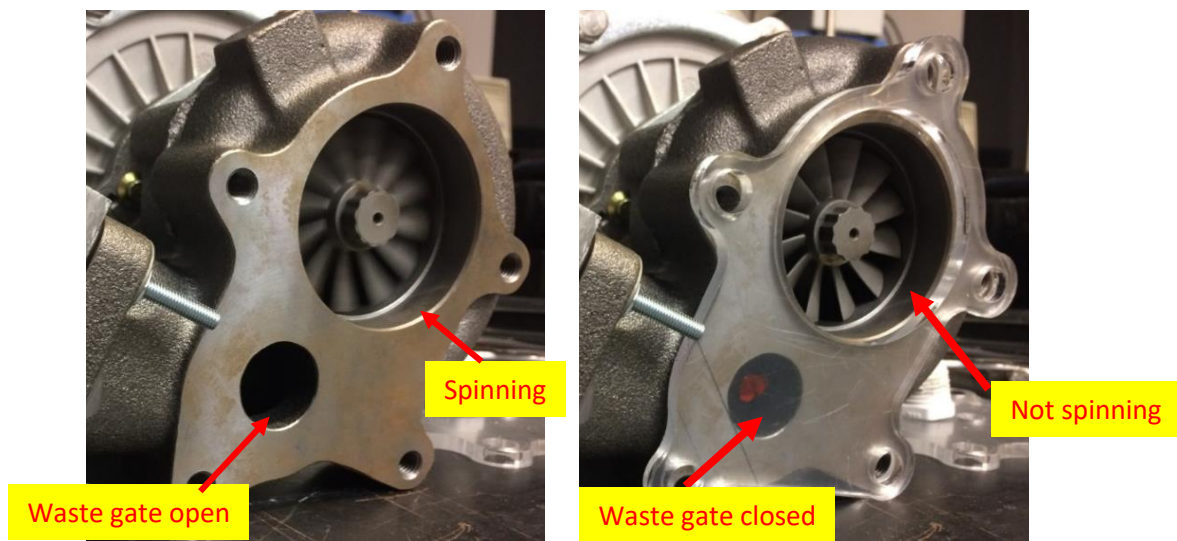
Figure 36: Turbine wheel rotation & Waste gate

After careful observations here is the conclusion

- Compressed air is not enough to build pressure inside turbine housing
- Waste gate is behaving as suction instead of releasing air outside due to low pressure in volute.
- If it would have enough pressure, then waste gate will behave as by pass valve otherwise waste gate is sucking air inside volute due to insufficient pressure
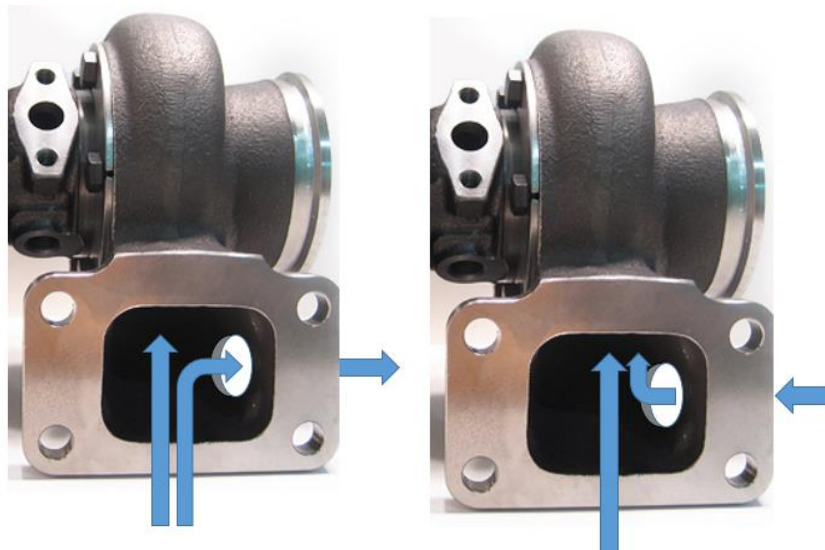
Figure 37: Flow behavior in turbine section

In order to rotate turbine wheel, some of different techniques were applied which are as follows.

6.4.2.1. Turbine Section Inlet

Turbine section inlet pictorial representation is given in Fig. 38. In Technique A, a simple kind of fitting was used to spread out flow to enhance effective area at turbine inlet. Technique B is similar to previous one but it has longer tube to stable air flow. In order to maximize tube length in technique C, fitting was departed to some distance to observe changes. It helped partially to rotate turbine wheel. In technique D, air flow was given at turbine inlet without spreading, it rotated turbine wheel. In Technique E, two inlets were used to observe turbine wheel rotation and it was successful most of the time.
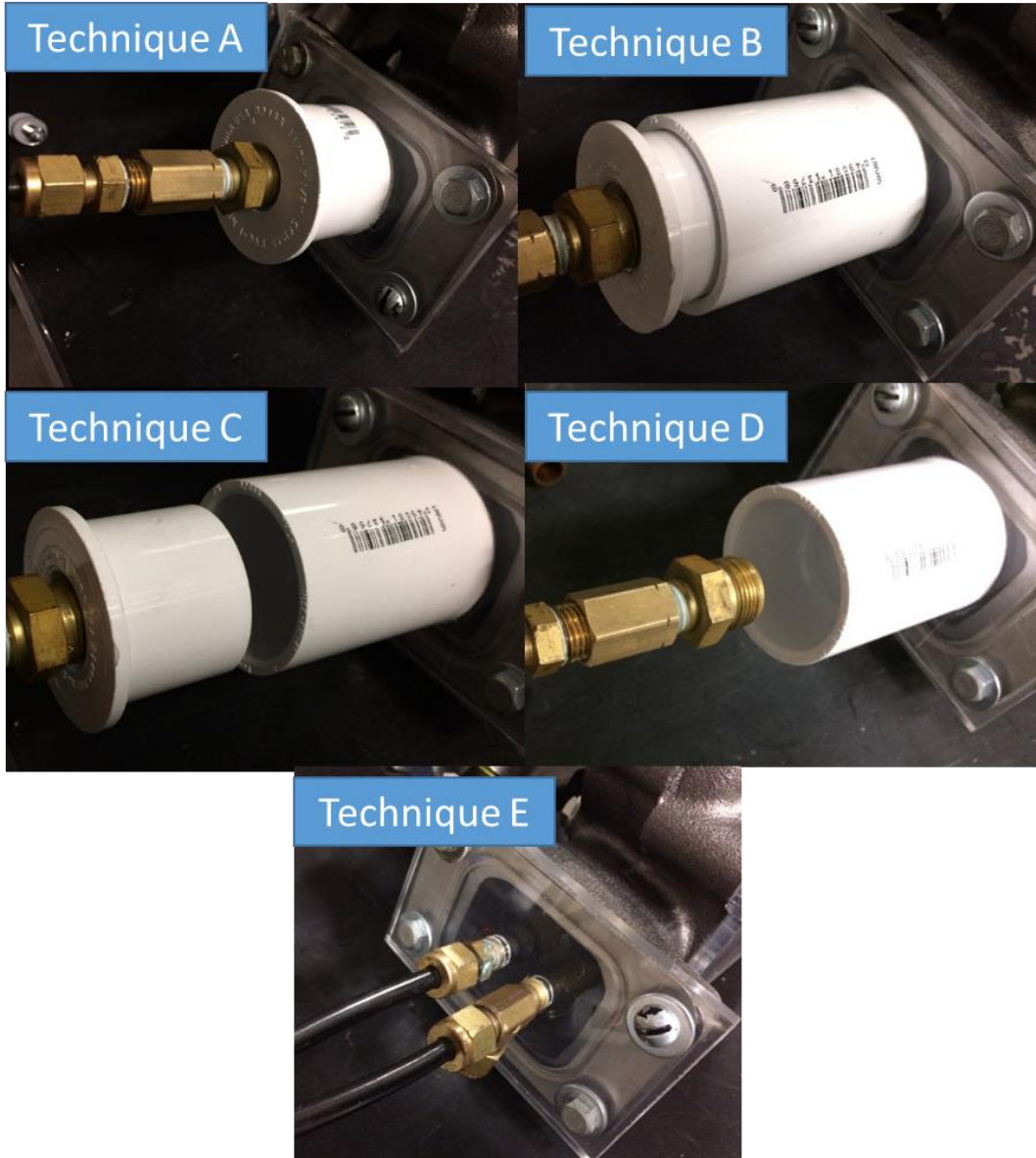
Figure 38. Techniques to inject compressed air in turbine section

6.4.2.2. Turbine Section Outlet

Customized fitting was used to measure pressure reading at outlet of turbine but it stopped turbine wheel due to surging as shown in Fig. 39. Hence it is to be noted that turbine outlet should be big enough to maintain continuous flow.

6.5. Manual Cranking

Initially hand cranking manually was suggested and tried with the help of had drill with star connection that can be fixed on the shaft of turbine. But it was noted that it is unable to produce
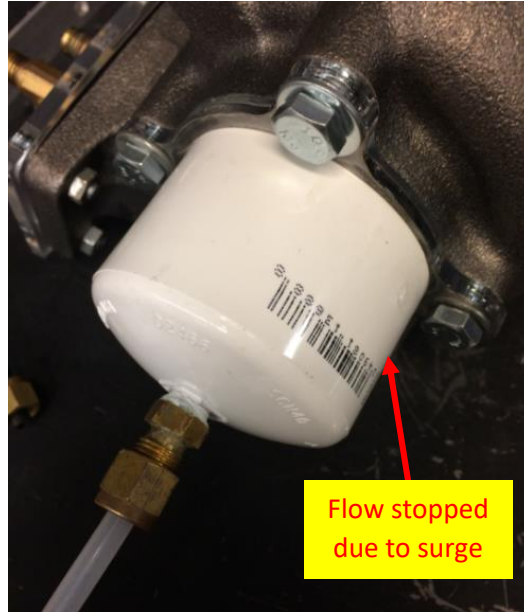
Figure 39: Turbine outlet flange

such pressure and air flow on which we can combust our fuel in side combustion chamber. Because no pressure was observed inside combustor on manual cranking.

6.5.1. Results

These are the results which we measured from above observations. Only **technique E** was turned out to be successful and its upstream and downstream pressures are given below. Pressure were noted for upstream and downstream as 32 Psi and 18.8 Psi respectively.

Techniques	A		B		C		D		E	
Readings	V	PSI	V	PSI	V	PSI	V	PSI	V	PSI
Upstream	0.86	14.4	1.35	34	0.85	14.2	1.3	32	1.34	33.6
Downstream	0.85	14.2	0.85	14.2	0.85	14.2	0.85	14.2	0.97	18.8

Table 3: Pressure Readings on Turbine Section
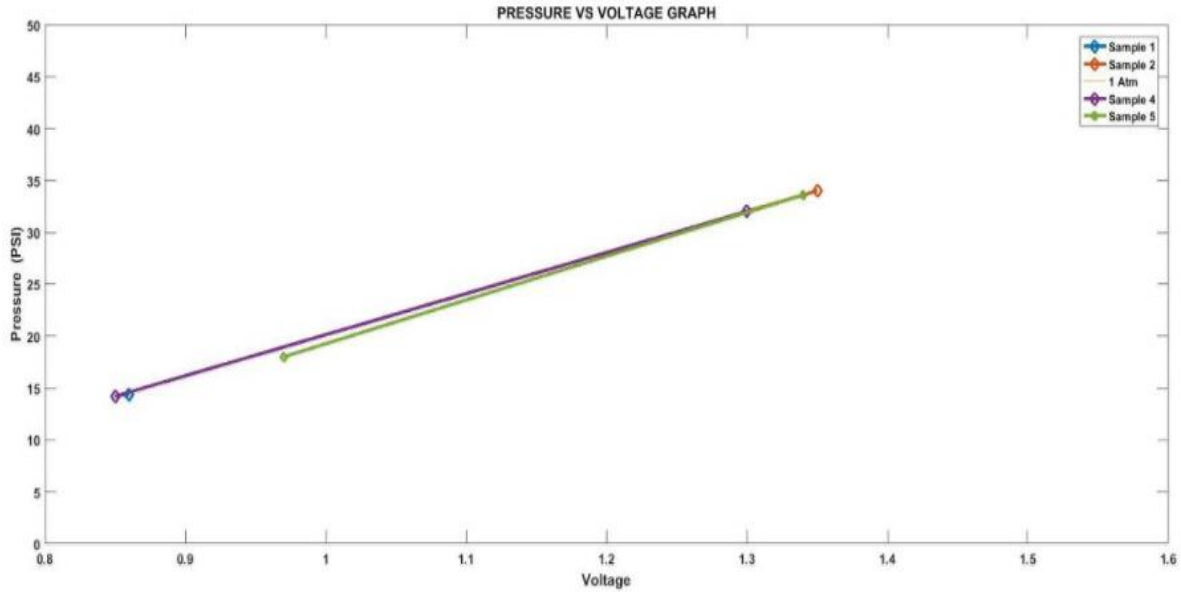
Figure 40: Graph for pressure readings on turbine section

6.6. Future Experimental Work

Micro Gas Turbine requires some modification to start properly

- Fuel Line Injection near spark ignition
- Lubrication System for turbocharger bearings

Parameters to be studied

- Flowrate Measurements
- Temperature
- Pressure
- RPM Reading by Tachometer
- Emission Measurement

Shaft Power

- Torque measurement through shaft will lead to calculate Power of Turbocharger will produce
- Torque cell can be used to calculate

Electricity Generation

- Connection of Turbocharger shaft can turn Electric Generator

Summary

From all observations and results from experimental work., it's been concluded as;

- Air Pressure should be enough to rotate turbine wheel
- For start-up of MGT, a compressed air inlet has been setup on combustor inlet so that combustion can take place easily.
- Manual cranking through hand drill has not applicability
- MGT is ready to start unless fuel injection tube arrives.

CONCLUSION AND RECOMMENDATIONS

MGT design has been established with battery sizing and charging configuration as mentioned in results section. Future work will be done to validate our study by comparing it with the size (volume and weight) of micro turbine engine.

In this study, the 85 kWh battery bank used by Tesla Model S P85D has been replaced by a 22 kWh capacity battery bank in order to achieve driving range of 100 km. The driving range limit has been set according to average driving requirement of vehicles. Overall battery pack weight has been reduced to 130 kg. For this particular case, a 47 kW MGT engine is required as an on-board charging device or range extender with an approximate efficiency of 33.4%. Charging time for batteries is approximated to be around 30 minute. A unique aspect of the aforementioned study is that the MGT design has been established in combination with battery sizing and charging configuration.

Future Work

MGT designs available in the market currently present a compact and integrated design of all its components in order to improve the MGT efficiency and operation in conventional recuperated brayton cycle. However, this acts against the ability of the MGT to be integrated or hybridized with other technologies, making it more complex and expensive to open and modify the cycle. Therefore, there is a particular need to design MGT for integration in order to increase the flexibility of the system regarding the cycle.

This work can lead to design and development work in Pakistan. Commercialization of this work will help industries to build light weight vehicles. Further development will lead to have higher electrical efficiency by designing Alternator according to MGT's specification. It will enhance overall efficiency.

Techno Economic Analysis

Electric vehicle batteries are characterized by a limited lifetime based on the steadily decreasing ability to fulfil the minimum capacity and power requirements for the automotive application.

Technical assessment has been done to estimate total weight of car with and without MGT. Total curb weight of Tesla P85D is around 2240 kg. By replacing 85 kWh battery pack with 23 kWh battery pack allowing vehicle to reduce its weight to 1830 kg. After addition of MGT, its total weight is coming out to be 1975 kg as shown in Table 4.

Category	Weight of Car [kg]	Weight of batteries [kg]	Weight of MGT [kg]	Total weight [kg]
Tesla P85d	1699	540	x	2239
Hypothesis	1699	130.6	145	1974.6

Table 4 Weight Analysis

While talking about economic analysis, it has been observed that capital / replacing cost of batteries and MGT are 84000 Rs/kWh and 98000 Rs/kWh respectively. This study is further divided into following sub categories.

Running Cost

As already discussed, our hypothesis model can give 100 km in one charging with energy of 23 kW which costs 485 rupees. While as Tesla Model P85S costs Rs. 2850 to drive 425 km. The projection of hypothesis model has been estimated to drive 425 km by charging its batteries through MGT which costs Rs. 2064 of fuel as shown in Table 5..

Tesla Model S					Basic Model for 100 kms				
[$/kWh]	[rs/kWh]	Energy Req [kW]	[rs]	[km]	SFCshaft [kg/kWh]	Energy Req [kWh]	Total Fuel [kg]	Unit price [rs/kg]	Total Price [rs]
0.24	33.6	85	2856	425	0.249	23	5.72	85	485.85
					Basic Model estimated for 425 km range				
					SFCshaft [kg/kWh]	Energy Req [kWh]	Total Fuel [kg]	Unit price [rs/kg]	Total Price [rs]
					0.249	97.75	24.29	85	2064.88

Table 5 Running cost analysis

Battery Replacing Cost

Tesla Model P85d has 85 kW battery size. Its maintenance cost is very high due to huge number of battery cells. Its battery bank consists of 7100 cells. Its battery cost is around Rs 71.4 Lac. Our

hypothesis model battery specified as 23 kW and its cost is around Rs 19.3 Lac. Hence its cost is 1/4th of actual size of tesla model as shown in Table 6.

Tesla Model S				Basic Model for 100 kms			
Battery Energy [kWh]	Cost per kWh [$]	Total Cost [$]	Total Cost Rs	Battery Energy [kWh]	Cost per kWh [$]	Total Cost [$]	Total Cost Rs
85	600	51000	7140000	23	600	13800	1932000

Table 6 Battery Cost Analysis

Vehicle Cost

Market price of Tesla Model is around Rs. 14 million. It is reduced to Rs 12 million. MGT manufacturing is one of challenging goal in this development. Difference of both models is not that significant due to MGT manufacturing cost as of yet. But its development is in progress and expected to be reduced in upcoming years. This will allow us to have economical and affordable MGT range extended vehicle for our daily use.

Appendix A

Appendix A contains all the design data of Capstone C30.

A.1. GSP Model Initial Conditions

Static/Total Ambient Conditions	Combustor
$P_{s,t} = 101,325 Pa$	Fuel flow $(W_f) = Variable$
$T_{s,t} = 288.15 K$	Exit temperature $(T_3) = Variable$
Relative humidity = 60%	Design combustion efficiency = 0.999 [−]
Load	Design point rel. pressure loss = 0.0200 [−]
Design Power = 30kW	**Turbine**
Inlet	Design rotor speed = 96164.50 [rpm]
Design mass flow = 0.313302 [$\frac{Kg}{s}$]	Design efficiency = 82%
	Expansion heat loss fraction = 0.50 [−]
Pressure ratio = 1 [−]	Tip diameter: 16.95cm
Compressor	Nsc = 0.707
Design Rotor Speed = 96,164.5 [rpm]	**Spool**
Design Pressure Ratio = Variable	Spool inertial moment = 0.7578 [kgm^2]
Design Efficiency = 75 %	Spool mechanical efficiency = 0.980 [−]
Heat transfer fraction = 0.50 [−]	**Exhaust**
Tip Diameter: 14.7cm	Velocity coefficient CV = 1.0 [−]
Recuperator	Thrust coefficient CX = 1.0 [−]
Effectiveness = 0.83 [−]	Throat CD = 1.0 [−]
Rel. total pressure loss:	**Duct**
Flow 1 = 0.015 [−]	Heat flux (input) = 3.14995 [kW]
Flow 2 = 0.040 [−]	Relative total pressure loss = 0 [−]

Table 7. Design Conditions

Table 7 shows all design conditions of each components. These values are taken from Capstones C30 microturbine to simulate the model with the most accurate conditions.

A.2. Performance Parameters

The following performance parameters are the official published performance data for Capstones C30 micro gas turbine seen in Table 8.

Capstone C30	
Output power (kW)	27
Electrical efficient (%)	26.1 (± 2)
Mass flow rate (kg/s)	0.31
Pressure ratio	3.5
Axial speed (rpm)	96,164.5
TIT ($°C$)	840
Exhaust Temperature ($°C$)	275
Fuel	Gaseous Propane/ Natural Gas/Diesel

Table 9. Capstone C-30 output performance data

It is stated here purely as a comparative medium for the data which was simulated by the models. A majority of the values, especially the thermal efficiency, are rated slightly higher than the experimental values calculated. This is possibly due to more accurate results obtained by test rig analysis. From this table and my graphs, it is possible to see that the data corresponds fairly accurately and that the C30 recuperated MGT is still only touching the beginning of the performance curves.

Appendix B

This appendix includes MGT design output data from GSP software.

GSP Output file (Preliminary Design of MGT)								
W	PR_c	TT5	WF	PWshaft	SFCshaft	Battery Energy	Battery Weight (Kg)	Charging Time (min)
0.4	3	1200	0.00265	36.98	0.26	17.26	100.74	28.00
0.4	3.5	1200	0.002886	40.17	0.26	18.74	109.40	28.00
0.4	4	1200	0.003078	42.15	0.26	19.67	114.81	28.00
0.4	4.5	1200	0.003243	43.31	0.27	20.21	117.97	28.00
0.4	5	1200	0.003398	43.88	0.28	20.48	119.52	28.00
0.4	5.5	1200	0.003524	44.00	0.29	20.53	119.86	28.00
0.4	6	1200	0.003636	43.79	0.30	20.44	119.28	28.00
0.4	3	1220	0.002709	38.72	0.25	18.07	105.47	28.00
0.4	3.5	1220	0.002949	42.15	0.25	19.67	114.81	28.00
0.4	4	1220	0.003145	44.34	0.26	20.69	120.78	28.00
0.4	4.5	1220	0.003313	45.68	0.26	21.32	124.43	28.00
0.4	5	1220	0.003473	46.41	0.27	21.66	126.42	28.00
0.4	5.5	1220	0.003602	46.68	0.28	21.78	127.14	28.00
0.4	6	1220	0.003716	46.59	0.29	21.74	126.91	28.00
0.4	3	1240	0.002769	40.46	0.25	18.88	110.20	28.00
0.4	3.5	1240	0.003013	44.13	0.25	20.60	120.22	28.00
0.4	4	1240	0.003213	46.54	0.25	21.72	126.76	28.00
0.4	4.5	1240	0.003398	48.07	0.25	22.43	130.93	28.00
0.4	5	1240	0.003548	48.95	0.26	22.84	133.33	28.00
0.4	5.5	1240	0.003679	49.35	0.27	23.03	134.43	28.00
0.4	6	1240	0.003796	49.40	0.28	23.05	134.55	28.00
0.4	3	1260	0.002828	42.20	0.24	19.69	114.94	28.00
0.4	3.5	1260	0.003078	46.12	0.24	21.52	125.63	28.00
0.4	4	1260	0.003284	48.74	0.24	22.74	132.75	28.00

0.4	4.5	1260	0.00347	50.45	0.25	23.54	137.41	28.00
0.4	5	1260	0.003624	51.49	0.25	24.03	140.25	28.00
0.4	5.5	1260	0.003758	52.03	0.26	24.28	141.73	28.00
0.4	6	1260	0.003877	52.20	0.27	24.36	142.20	28.00
0.4	3	1280	0.002888	43.94	0.24	20.51	119.68	28.00
0.4	3.5	1280	0.003143	48.11	0.24	22.45	131.05	28.00
0.4	4	1280	0.003367	50.95	0.24	23.78	138.77	28.00
0.4	4.5	1280	0.003543	52.83	0.24	24.65	143.90	28.00
0.4	5	1280	0.003699	54.03	0.25	25.21	147.17	28.00
0.4	5.5	1280	0.003836	54.72	0.25	25.54	149.04	28.00
0.4	6	1280	0.003958	55.02	0.26	25.67	149.85	28.00
0.4	3	1300	0.002948	45.68	0.23	21.32	124.43	28.00
0.4	3.5	1300	0.003208	50.10	0.23	23.38	136.47	28.00
0.4	4	1300	0.003437	53.15	0.23	24.80	144.77	28.00
0.4	4.5	1300	0.00362	55.22	0.24	25.77	150.40	28.00
0.4	5	1300	0.003776	56.57	0.24	26.40	154.10	28.00
0.4	5.5	1300	0.003916	57.41	0.25	26.79	156.36	28.00
0.4	6	1300	0.00404	57.83	0.25	26.99	157.52	28.00

Table 10. GSP Output File (Preliminary Design of MGT)